HHS Public Access

Author manuscript

Cell Rep. Author manuscript; available in PMC 2022 April 29.

Published in final edited form as:

Cell Rep. 2022 March 29; 38(13): 110567. doi:10.1016/j.celrep.2022.110567.

Pathogen size alters C-type lectin receptor signaling in dendritic cells to influence CD4 Th9 cell differentiation

Seeun Oh[1,2,3], **Kai Li**[1,2], **Alexander Prince**[1,2], **Matthew L. Wheeler**[1,2], **Hussein Hamade**[1,4], **Christopher Nguyen**[1,2], **Kathrin S. Michelsen**[1,2,4], **David M. Underhill**[1,2,3,4,5,*]

[1]F. Widjaja Foundation Inflammatory Bowel & Immunobiology Research Institute, Cedars-Sinai Medical Center, 8700 Beverly Blvd., Los Angeles, CA 90048, USA

[2]Research Division of Immunology, Department of Biomedical Sciences, Cedars-Sinai Medical Center, Los Angeles, CA 90048, USA

[3]Graduate Program in Biomedical Sciences, Cedars-Sinai Medical Center, Los Angeles, CA 90048, USA

[4]The Karsh Division of Gastroenterology and Hepatology, Department of Medicine, Cedars-Sinai Medical Center, Los Angeles, CA 90048, USA

[5]Lead contact

SUMMARY

Dectin-1 recognizes β-glucan in fungal cell walls, and activation of Dectin-1 in dendritic cells (DCs) influences immune responses against fungi. Although many studies have shown that DCs activated via Dectin-1 induce different subsets of T helper cells according to different cytokine milieus, the mechanisms underlying such differences remain unknown. By harnessing polymorphic *Candida albicans* and polystyrene beads of different sizes, we find that target size influences production of cytokines that control differentiation of T helper cell subsets. Hyphal *C. albicans* and large beads activate DCs but cannot be phagocytosed due to their sizes, which prolongs the duration of Dectin-1 signaling. Transcriptomic analysis reveals that expression of *Il33* is significantly increased by larger targets, and increased IL-33 expression promotes T_H9 responses. Expression of IL-33 is regulated by the Dectin-1-SYK-PLCγ-CARD9-ERK pathway. Altogether, our study demonstrates that size of fungi can be a determining factor in how DCs induce context-appropriate adaptive immune responses.

*Correspondence: david.underhill@csmc.edu.

AUTHOR CONTRIBUTIONS

Conceptualization, S.O., M.L.W., K.S.M., and D.M.U.; methodology, S.O., M.L.W., H.H., and K.S.M.; investigation, S.O. and K.L.; resources, A.P. and C.N.; writing – original draft, S.O. and D.M.U.; writing – review & editing, S.O., K.L., K.S.M., and D.M.U.; funding acquisition, D.M.U.

DECLARATION OF INTERESTS

The authors declare no competing interests.

SUPPLEMENTAL INFORMATION

Supplemental information can be found online at https://doi.org/10.1016/j.celrep.2022.110567.

SUPPORTING CITATIONS

The following references appear in the supplemental information: Gorski et al. (2013); Hori et al. (2010); Spadoni et al. (2012); Takedatsu et al. (2008).

In brief

Oh et al. show that dendritic cells exposed to C. *albicans* hyphae more strongly induce IL-9-producing T cells compared with cells exposed to yeast. They find that this T_H9 response is driven in large part by Dectin-1 sensing microbe size, leading to elevated production of IL-33.

Graphical Abstract

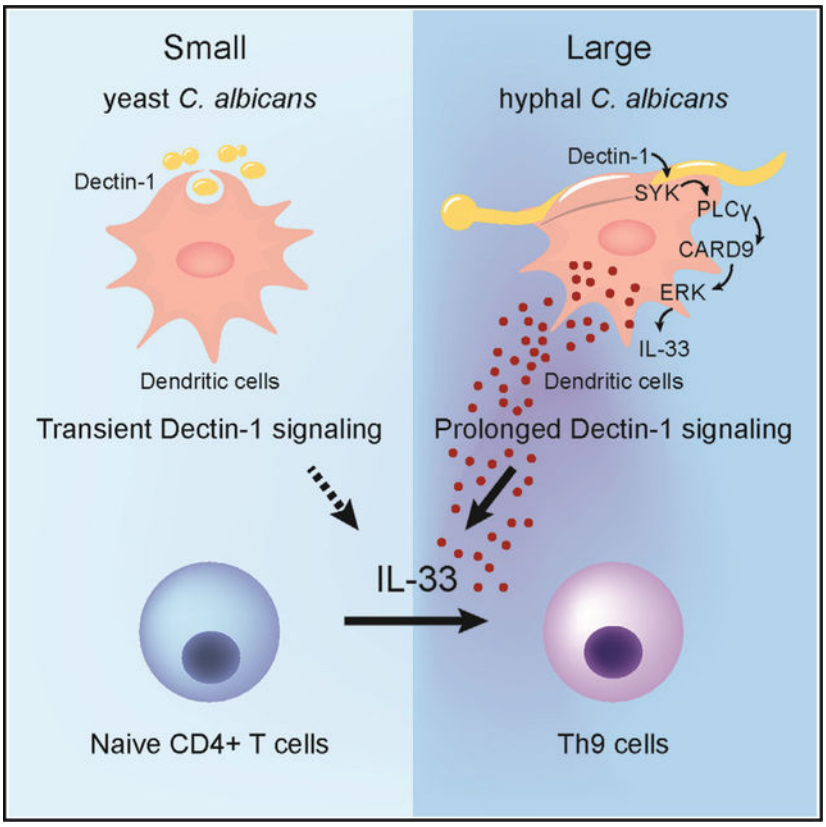

INTRODUCTION

Candida albicans is an opportunistic commensal fungus, which can cause a life-threatening infection in people with weakened immunity or other predispositions (Wisplinghoff et al., 2014). *C. albicans* can switch morphologies from yeast to hyphal filaments in response to environmental signals such as alterations in nutrition, temperature, pH, or oxygen (Whiteway and Oberholzer, 2004). This organism is a common commensal resident of the mammalian gastrointestinal tract where it is subject to diverse environmental and immunological stimuli. While the yeast form is generally thought of as the predominant commensal form (Vautier et al., 2015; White et al., 2007), studies have shown that hyphal forms also occur in the murine intestine (Ost et al., 2021; Witchley et al., 2019).

Different morphologies of *C. albicans* induce different immune responses (Gantner et al., 2005; Lowman et al., 2014; Mukaremera et al., 2017; Wheeler et al., 2008). Dendritic cells (DCs) recognize different morphologies of *C. albicans* and differentiate context-appropriate

subsets of T helper (T_H) cells to orchestrate immune responses (d'Ostiani et al., 2000; Kashem et al., 2015). Evidence that different morphologies of *C. albicans* stimulate different pattern-recognition receptors (PRRs) on DCs (Gantner et al., 2005; Lowman et al., 2014; Mukaremera et al., 2017; Wheeler et al., 2008), and studies that have shown that different subsets of DCs induce specific subsets of T_H cells (Igyarto et al., 2011; Kashem et al., 2015), highlight the complexity of factors that influence DC regulation of T_h cell polarization. In addition, the size of the target also shapes DC trafficking, processing, and presentation of antigens, which are all factors that can influence T cell fate (Joshi et al., 2013; Mant et al., 2012; Tran and Shen, 2009). For example, DCs induce T_H1 responses when stimulated with large (~1,000 nm) and small (~250 nm) particles loaded to a high density with CpG. In contrast, smaller particles loaded with less CpG induce primarily T_H2 responses (Leleux et al., 2017). Similarly, at least one paper has suggested that large aggregated glucan stimulates increased secretion of interleukin (IL)-1β, IL-6, and IL-23 from DCs compared with smaller glucan-coated microparticles (Elder et al., 2017). With regards to the handling of internalized particles, one study suggests that DCs more efficiently process antigens from smaller-sized particles for cross presentation and induction of $CD8^+$ T cell responses compared with larger particles (Joshi et al., 2013). While these data support the idea that DC responses to microbes are influenced by diverse factors, the factors specifically contributing to differential DC responses to *C. albicans* yeast and hyphae in T_H cell polarization remain to be defined.

C-type lectin receptors (CLRs), which recognize carbohydrate structures, play a central role in immunity to fungi. Dectin-1 is a key CLR that has been shown to have critical roles in antifungal immunity through recognizing β(1→3)- and/or β(1→6)-linked glucan, which is one of the major components of fungal cell walls (Brown and Gordon, 2001). Dectin-1 is mainly expressed on myeloid cells, and its activation triggers production of pro-inflammatory cytokines that influence an ensuing immune response (Brown et al., 2003; Goodridge et al., 2007). Dectin-1 transduces signals through pathways involving spleen tyrosine kinases (SYKs) and the serine threonine kinase Raf-1. Phosphorylation of SYK leads to activation of several downstream, often cross-interacting signaling pathways, involving phospholipase Cγ2 (PLCγ2), c-Jun N-terminal kinase (JNK), p38, and extracellular-signal-regulated kinase (ERK) and mitogen activated protein (MAP) kinase, reactive oxygen production, protein kinase C delta (PKCδ), nuclear factor of activated T cells (NFAT), and a signaling complex including CARD9, Bcl10, and MALT1 that coordinates, among other signals, activation of nuclear factor κB (NF-κB) (Vornholz and Ruland, 2020). Activation of Dectin-1 in DCs can drive them to induce a variety of subsets of $CD4^+$ T_h cells, including T_H1, T_H2, T_H9, or T_H17, depending on the situation (Gringhuis et al., 2009; Kashem et al., 2015; LeibundGut-Landmann et al., 2007; Zhao et al., 2016). However, how Dectin-1 signaling activates DCs to induce distinct $CD4^+$ T_H subsets remains to be fully understood.

In addition to T_H17 cells, IL-9 is mainly produced by T_H9 cells that are now considered a distinct subset of T_H cells (Dardalhon et al., 2008; Veldhoen et al., 2008). Previous studies have revealed that T_H9 cells contribute to pathogenesis of inflammatory diseases, such as allergic lung inflammation and inflammatory bowel disease (IBD) (Gerlach et al., 2014; Jones et al., 2012; Sehra et al., 2015), and exhibit strong anti-cancer activities

(Angkasekwinai and Dong, 2021; Rivera Vargas et al., 2017). Recent studies indicate that Dectin-1 activation in DCs can promote the induction of T_H9 cells by increasing DC expression of co-stimulatory molecules tumor necrosis factor (TNF) superfamily member 15 (TNFSF15) and TNF superfamily member 4 (OX40L) and secretion of IL-33 (Chen et al., 2018; Zhao et al., 2016), suggesting that T_H9 cells may play a role in antifungal immunity. Although the potential role of T_H9 cells in antifungal immunity is poorly understood, human skin memory T_H9 cells have been shown to be specific for *C. albicans* and to modulate the effector functions of other subsets of T_H cells through paracrine effects of IL-9 (Schlapbach et al., 2014). Similarly, /*l9r*-deficient mice have been shown to have decreased production of inflammatory cytokines in the stomach early in the course of *C. albicans* infection (Renga et al., 2018). However, studies have not been conducted to determine whether T_H9 cells are induced in response to *C. albicans* regardless of morphology.

IL-33 is an alarmin that is released extracellularly when cells are damaged, triggering a strong immune response. IL-33 is known to induce type 2 immune responses by activating the IL-33 receptor ST2 expressed on mast cells, macrophages, DCs, innate lymphoid cells type 2 (ILC2s), regulatory T (T reg) cells, and T_H2 cells (Liew et al., 2016; Molofsky et al., 2015). However, recent studies have shown that IL-33 also enhances T_H9 polarization by activating ST2 expression in T_H cells (Chen et al., 2018; Ramadan et al., 2017) and by stimulating DCs to increase the expression of OX40L (de Kleer et al., 2016), a co-stimulatory molecule that also promotes T_H9 differentiation (Xiao et al., 2012).

In this study, we found that DCs exposed to *C. albicans* hyphae preferentially induce T_H9 responses compared with yeast. RNA sequencing (RNA-seq) analysis revealed that there is a different transcriptional profile induced according to the size of target and that the differences include factors known to be involved in polarizing T_H9 cells. This response was triggered through Dectin-1 and, specifically, by Dectin-1 activated by physically large, hyphae-sized surfaces. We observed that stimulation of DCs with large targets augments the duration of Dectin-1 signaling and increases expression of *Il33.* Optimal hyphae-induced DC polarization of T_H9 cells via Dectin-1 required the production of IL-33. This study indicates that the size of fungi can act as a determinant in shaping the immune response to the fungi.

RESULTS

Activation of DCs with filamentous *C. albicans* induces T_H9 response

To explore whether *C. albicans* morphology might influence how DCs direct T_H differentiation, we stimulated DCs overnight with paraformaldehyde (PFA)-fixed *C. albicans* genetically engineered to be locked in the yeast form *(efg1/cph1,* yeast locked) or the filamentous form *(nrg1,* hyphal locked), which were normalized to the dry weight of material. We then pulsed the cells with ovalbumin (Ova) peptide 323–339 prior to co-culture with naïve $Rag^{-/-}$ OT-II $CD4^+$ T cells without further addition of polarizing cytokines (Figure 1A). We assessed T cell differentiation after 3 days by measuring production of interferon (IFN)γ, IL-4, IL-9, IL-13, and IL-17 in the co-culture media by ELISA. We did not observe any measurable secretion of IL-4 and IL-17 in samples where DCs were stimulated with yeast-locked *C. albicans* (YLCA) or with hyphal-locked *C. albicans* (HLCA) (data not shown), and we observed no significant differences in IFNγ

production between YLCA and HLCA (Figure 1B). Although HLCA stimulation drove more production of IL-13 from DCs than YLCA, they were not significantly different when compared with unstimulated controls. Notably, production of IL-9 was significantly increased in co-culture supernatants from DCs stimulated with HLCA compared with YLCA (Figure 1B). This was particularly interesting because in most studies of T_H9 polarization, T cells must be additionally cultured with T_H9-polarizing cytokines such as transforming growth factor β (TGF-β) and IL-4 (Dardalhon et al., 2008; Xiao et al., 2012). Our data demonstrate that *C. albicans* hyphae are sufficient to direct T_H9 polarization without additional cytokine supplementation.

We next confirmed that both forms of the fungi can be recognized by DCs and activate downstream signaling. We stimulated DCs with YLCA or HLCA and immunostained the DCs for phosphorylated SYK (pSYK). As previously reported, we observed that DCs can recognize both morphologies of *C. albicans* and activate SYK in response, which is a well-known downstream protein of CLRs (Underhill et al., 2005) (Figure 1C). Furthermore, we observed production of the pro-inflammatory cytokines TNFα and IL-6 in DCs stimulated with either YLCA or HLCA (Figure S1A). This suggests that the lack of a T_H9 response in YLCA-stimulated DCs may be due to the generation of a different cytokine milieu between YLCA- or HLCA-stimulated DCs, not due to insufficient stimulation of DCs. To exclude any possible effects specific to our engineered strains, we repeated the experiment with a wild-type strain of *C. albicans,* SC5314, grown as yeast or hyphae under different culture conditions. Consistent with the mutant strains, DCs stimulated with hyphal *C. albicans* specifically induced IL-9 production in co-cultures compared with DCs stimulated with *C. albicans* yeast or lipopolysaccharide (LPS) (Figure 1D). To exclude the possibility that T_H9 polarization might be specific to OT-II cells or related to alterations in DC antigen processing, we repeated the co-culture experiment using wild-type naive T_H cells and anti-CD3/anti-CD28 stimulation to differentiate T cells in the presence of YLCA- or HLCA-stimulated DCs. Consistently, DCs stimulated with hyphae significantly supported a T_H9 response in the co-culture without supplementing additional cytokines (Figure 1E). Together, these results indicate that filamentous *C. albicans* drives DCs to produce a cytokine milieu that promotes T_H9 responses, while yeast do not.

T_H9 polarization by DCs stimulated with large targets is Dectin-1 dependent

C. albicans yeast and hyphae can be recognized by different innate PRRs on phagocytic cells (Gantner et al., 2005; Sato et al., 2006), and they are vastly different in size. We therefore considered the possibility that differential T_H cell polarization of DCs to yeast and hyphal forms of *C. albicans* is due to the activation of a different combination of PRRs or that it might be due to the different sizes of the two morphological forms. While Dectin-1 is known to be an important receptor for recognizing β-glucan on *C. albicans,* exposure of β-glucan, and thus recognition by Dectin-1, may vary between strains and morphologies (Gantner et al., 2005; Marakalala et al., 2013; Wheeler et al., 2008). To investigate whether Dectin-1 could recognize the strains of *C. albicans* we have used thus far, we stained both forms of fungi with soluble a murine Dectin-1 receptor fused with human immunoglobulin G (IgG)1 Fc domain according to methods previously described (Graham et al., 2006). We observed that both YLCA and HLCA were recognized by Dectin-1 (Figure 2A). To further understand

the role of CLR pathways in recognizing the strains and driving T_h9 polarization, we compared wild-type DCs with cells deficient in Dectin-1 *(Clec7a)* or Dectin-2 *(Clec4n).* We observed that T_h9 polarization was significantly reduced when using Dectin-1-deficient DCs (Figure 2B) but not in Dectin-2-deficient DCs (Figure 2C). Consistent with the importance of the CLR pathway in T_H9 polarization, we also found that DCs lacking the key CLR pathway signaling protein CARD9 could not support the hyphal-induced T_H9 response (Figure 2D).

These data suggest that Dectin-1/CARD9 signaling may be sufficient to direct the T_H9 response, but if so, the hyphal context of the signal should be important compared with the yeast. We therefore directly examined the effect of particle size on Dectin-1 activation and T_H9 polarization. We stimulated DCs with various sizes of polystyrene beads (diameters of 3–45 μm) passively coated with β-glucan (Dectin-1 ligand), mannan (Dectin-2 or mannose receptor ligand), or with BSA as a control. For the bead stimulation, we used 10 particles of 3 μm beads per DC and normalized the number of beads of different sizes to have equivalent total surface areas. Interestingly, bead-stimulated DCs induced T_H9 responses in co-culture assays only when stimulated with β-glucan-coated beads of 15 μm or larger (Figure 2E). Beads of 15 μm are substantially larger than *C. albicans* yeasts (5–6 μm), and beads of this size begin to become difficult for DCs to internalize, thereby multiple DCs cover the surface of a large bead (Figure 2F). While the large beads are not internalized due to their large diameter, hyphae are similarly not able to be internalized, but this is due to their extended length. The inability of the small-bead-stimulated DCs to induce a T_H9 response was not due to poor coating or engagement with DCs since both β-glucan and mannan-labeled beads induced an oxidative burst in DCs to a similar degree as *C. albicans* yeast (Figure S1B).

C. albicans mutants locked in yeast or hyphal form are deleted for transcription factors that might differently regulate expression of proteins that are additionally important for the propensity to promote DCs to drive Th9 polarization. To examine this directly, we prepared *C. albicans* hyphae and mechanically fragmented them into pieces sufficiently small to be phagocytosed but having the same molecular composition as the hyphae. We observed that while full-length hyphae strongly promote DCs to support Th9 polarization of T cells, the fragmented hyphae were significantly reduced in their ability to do so (Figure 2G).

Together, these results suggest that Dectin-1 signaling in response to large targets is different from Dectin-1 signaling induced by smaller particles and that this difference is related to the ability of larger particles and hyphae to specifically promote T_H9 responses.

Large targets induce prolonged Dectin-1 signaling in DCs

Internalization of Dectin-1 in DCs attenuates its downstream signaling pathway and minimizes production of pro-inflammatory cytokines (Hernanz-Falcon et al., 2009). Similarly, TLR4 internalization is associated with changes in signaling mechanisms (Cheng et al., 2015; Kagan et al., 2008). To determine if the duration of Dectin-1 signaling was affected by the differing forms of *C. albicans*, we compared the duration of Dectin-1 signaling in DCs stimulated with hyphae or yeast. First, we measured the internalization of Dectin-1 by immunocytochemistry and flow cytometry by measuring the expression of Dectin-1 on the surface of DCs. DCs stimulated with YLCA rapidly internalized Dectin-1

receptors after just 5 min of stimulation, but stimulation of DCs with HLCA was not associated with a similar loss of receptor from the cell surface (Figures 3A and 3B). Next, we measured the duration of Dectin-1 activation by measuring phosphorylation of SYK and ERK downstream of stimulation with YLCA or HLCA. DCs stimulated with YLCA rapidly phosphorylated downstream signaling proteins as early as 5 min, followed by a loss of signaling within 2 h of stimulation. However, stimulation of DCs with HLCA resulted in relatively slow phosphorylation of the downstream proteins that was maintained up to 6 h (Figure 3C). To determine whether Dectin-1 downstream signaling persists solely because of the size of the target, we stimulated DCs with β-glucan-coated 6 μm or 25 μm polystyrene beads and evaluated the phosphorylation of downstream proteins of Dectin-1. Similar to HLCA-stimulated DCs, large-bead-stimulated DCs showed prolonged Dectin-1 signaling compared with small-bead-stimulated DCs (Figure 3D). While these data suggest a difference in timing and cadence of Dectin-1 signaling in response to yeast and hyphae or small and large beads, the assays can be quite noisy. To directly test whether the length or persistence of Dectin-1 signaling is sufficient to instruct DCs to support T_H9 polarization or not, we developed an experimental approach in which we could specifically activate Dectin-1 signaling on DCs and experimentally control the length of the active signal. We utilized plates coated with β-glucan to synchronously activate Dectin-1 in DCs and a SYK inhibitor to shut down signaling from the receptor early, to mimic a short activation time, or not, to allow persistent signaling. The next day, we transferred the DCs to fresh plates without β-glucan or inhibitor and started the co-culture with naïve $CD4^+$ cells (Figure 3E). We observed a significant reduction of T_H9 response using DCs that had been treated with the SYK inhibitor (Figure 3F). Taken together, these findings suggest that alterations in the duration of Dectin-1 signaling contribute substantially to the discrimination of target size by DCs and influences the differentiation of T_h cell subsets.

Activation of Dectin-1 signaling by large particles induces genes associated with T_H9 polarization

As a first step toward characterizing the responses of DCs to large targets that might influence T_H9 differentiation, we employed RNA-seq to investigate the transcriptional changes in DCs stimulated overnight with 6 μm β-glucan-coated beads, 25 μm β-glucan-coated beads, PFA-fixed YLCA, or HLCA (Figure 4A). We compiled a list of differentially expressed genes, defined as >2-fold difference with a p value <0.05, between the larger and smaller pairs of stimuli (small: 6 μm β-glucan-coated beads and YLCA versus large: 25 μm β-glucan-coated beads and HLCA). Cluster analysis showed that DCs stimulated with 25 μm β-glucan-coated beads or HLCA had a similar gene signature compared with DCs stimulated with YLCA or 6 μm β-glucan-coated beads (Figure 4B). To identify the functionally relevant genes driving T_H9 differentiation in DCs stimulated with large targets, we compared differentially expressed genes based on the unstimulated control among the groups. Using a 2-fold cutoff and a p value <0.05, we identified 46 genes (31 up-regulated and 15 down-regulated) uniquely shared in DCs stimulated by the larger 25 μm β-glucan-coated beads and HLCA compared with the smaller stimuli (Figure 4C). Not unexpectedly, yeast and hyphae differentially regulated many genes that were not mimicked by the small and large β-glucan-coated beads. This indicates that many differences in immune responses elicited by yeast and hyphae cannot be explained by Dectin-1 signaling on small and large

particles. These differences could be due to differences in ligand expression or presentation by yeast and hyphae or due to differences in small-versus large-surface signaling via receptors other than Dectin-1. Many of these differences are undoubtedly important in defining how the immune response to *C. albicans* develops. However, for the purposes of this study, we focused on the 46 genes whose regulation was mimicked by the small and large β-glucan-coated beads since the signaling provided by the beads was minimally sufficient to replicate the differential induction of Th9 responses.

Among the 31 shared up-regulated genes, *Il33* and *Tnfsf15,* which are reported to have a role in T_H9 differentiation (Chen et al., 2018; Tsuda et al., 2019), were in the top 15 differentially expressed genes (Figure 4D). We then compared expression of genes that have been previously reported to be linked toT_H9 differentiation (Chen et al., 2018; Elyaman et al., 2012; Jiang et al., 2019; Karim et al., 2017; Liao et al., 2014a; Takami et al., 2012; Tan et al., 2014; Tsuda et al., 2019; Veldhoen et al., 2008; Xiao et al., 2012, 2015; Xue et al., 2019; Yao et al., 2013). As we expected based on the *in vitro* T cell polarization results, DCs stimulated with large targets had higher mRNA expression of genes, which can provide additional signals for T_H cells to polarize into T_H9 cells including *Il33, Tnfsf15,* and *Il1b,* than DCs stimulated with small targets (Figure 4E). We validated the data obtained from RNA-seq by qRT-PCR, confirming that selected genes reported to induce T_H9 polarization. We found that *Il33* and *Tnfsf15* were significantly increased specifically in DCs simulated with HLCA and the larger beads (Figure 4F), whereas the others, including *Tnfsf18, Tnfsf14,* and *Tslp,* were induced preferentially by hyphae but not as convincingly by larger beads.

Increased expression of *Il33* in large-target-stimulated DCs is regulated by Dectin-1 but not Dectin-2

Based on our RNA-seq data, genes involved in T_H9 polarization were significantly induced in DCs stimulated with large targets (Figure 4E). As T_H9 differentiation is Dectin-1 dependent (Figure 2B), we next asked if the increased expression of T_H9-associated genes *(Il33, Tnfsf15, Tnfsf18, Tnfrsf4,* and *Tslp)* was regulated by the Dectin-1. Wild-type DCs or Dectin-1-deficient DCs were stimulated with YLCA or HLCA, and gene expression was measured by qRT-PCR. We observed that increased expression of *Il33, Tnfsf15, Tnfsf18,* and *Tnfsf4* in wild-type DCs stimulated with HLCA was significantly reduced in Dectin-1 deficient DCs, while *Tslp* induction by HLCA was not dependent on Dectin-1 (Figure 5A). We next confirmed that the increased expression of T_H9-associated genes induced by the larger β-glucan-coated beads is mediated by Dectin-1. Consistent with the HLCA-stimulated DCs, induction of these genes by 25 μm β-glucan-coated beads was also lost in Dectin-1 deficient DCs (Figure 5B). Although we observed that Dectin-2 is not involved in hyphal-induced T_H9 polarization, we also tested the role of Dectin-2 in the induction of these additional candidate T_H9-inducing genes. We confirmed that induction of HLCA T_H9-associated genes in DCs is not regulated by Dectin-2 (Figure 5C). To determine whether PFA fixing YLCA or HLCA to prevent fungal overgrowth during DC stimulation might influence cell-wall structure in a way that might cause the observed differences in gene induction, we additionally compared the effects of heat killing of yeast and hyphae. Like the fixed *C. albicans,* we observed that heat-killed hyphae more potently induced *Il33* compared

with yeast (Figure 5D). Furthermore, to be sure that hyphae-induced *Il33* transcription corresponded to increased protein production, we performed ELISAs on cells stimulated with YLCA or HLCA or with 6 μm or 25 μm β-glucan-coated beads. In both cases, the larger stimuli induced more IL-33 protein production (Figure 5E).

IL-33 is a key cytokine that drives T_H9 polarization in DCs stimulated with large targets

Previously, Chen and colleagues reported that IL-33 produced by stimulation of DCs with curdlan, a crude β-glucan preparation purified from *Alcaligenes faecalis* that varies widely in size up to chunks greater than 500 μm (Rosas et al., 2008), potentiates T_H9 cell differentiation under T_H9-polarizing conditions requiring supplementation with TGF-β and IL-4 (Chen et al., 2018). We therefore asked whether the increased expression of *Il33* in DCs stimulated with *C. albicans* hyphae contributes to the specific T_H9 differentiation observed relative to yeasts. We knocked down *Il33* expression by transfecting DCs with small interfering RNA (siRNA) through electroporation. We tested the efficiency of four different siRNAs by measuring both gene expression and protein levels in DCs (Figures S2A and S2B). After we confirmed the efficiency of siRNA, we transfected DCs with *Il33* siRNA or scrambled siRNA prior to stimulation with YLCA or HLCA followed by pulsing with OVA peptide. Naïve $Rag^{-/-}$ OT-II $CD4^+$ T cells were co-cultured with overnight-stimulated and siRNA-transfected DCs. We observed a significant reduction of the T_H9 response in the co-culture of *Il33* siRNA-transfected DCs (Figures 6A and S2C). The T_H9 response was not completely lost, which may be due to additional factors that, together with *Il33*, support the polarization, or to residual *Il33* expression. To better understand which signaling pathways of Dectin-1 regulate the expression of *Il33*, we harnessed CARD9-deficient DCs or blocked Dectin-1 signaling in DCs 1 h before stimulation with various inhibitors of SYK (piceatannol), PLCγ2 (U73122), p38 (SB203580), or MEK1/2 (U0126) (Figure 6B). We tested whether the expression of *Il33* is regulated by CARD9 by using CARD9-deficient DCs. We observed a significant decrease of *Il33* expression in CARD9-deficient DCs (Figure 6C). Expression of *Il33* was significantly decreased in SYK, PLCγ2, and MEK1/2 inhibitor-treated DCs but not in p38 inhibitor-treated DCs (Figures 6D–6G), indicating that *Il33* expression is regulated by both CARD9-dependent and -independent pathways. Together, these data suggest that sustained signaling via the Dectin-1/SYK/PLCy2/CARD9/MEK axis promotes T_H9 differentiation at least in part through enhanced production of IL-33.

DISCUSSION

DCs have an important function in activating appropriate adaptive immunity by differentiating specific subsets of T_H cells, which is critical for efficient host protection during an infection. There is considerable evidence that DCs discriminate between different classes of pathogens by the types of PRRs that are engaged during an infection and that they use this information to ultimately dictate T_H cell differentiation. Here, we provide evidence that qualitative differences in “how” PRRs are engaged in DCs are additionally important for T_H cell polarization. While others have shown that DCs stimulated through Dectin-1 induce various different subsets of T_H cells (Gringhuis et al., 2009; Kashem et al., 2015; LeibundGut-Landmann et al., 2007; Zhao et al., 2016), data are scarce investigating

how DCs can be differentially activated via Dectin-1. In this study, we show that the size of fungi influences the stimulation of DCs through Dectin-1, thereby influencing T_H cell polarization.

Immune cells recognize a wide range of microbes of different shapes and sizes that express different PAMPs on their surfaces and induce an appropriate immune response based on the microbial information. Although there have been studies showing that DCs discriminate the morphology of *C. albicans* through activation of different PRRs (Kashem et al., 2015), the effect on the intrinsic size difference between yeast and hyphae has been less considered. Like pathogen-associated molecular patterns (PAMPs), target size also provides a layer of information that DCs can integrate to elicit context-appropriate immune responses. The inability to internalize targets via Dectin-1, due to either size constraints of the target (frustrated phagocytosis) or to pharmacological inhibition of phagocytosis, promotes sustained signal transduction and pro-inflammatory cytokine production by macrophages and DCs (Hernanz-Falcon et al., 2009; Rosas et al., 2008). It has also been shown that β-glucan size influences DCs in increasing specific cytokine secretion (Elder et al., 2017), which suggests that T_H cells can be differentiated into various different subsets of T_H cells depending on the size of target. We found that large targets induced prolonged Dectin-1 signaling in DCs, creating a different cytokine milieu between DC stimulated with large or small targets. Using different sizes of beads, we were able to activate DCs with targets via the same PRR but with differing sizes. We found that T_H9 polarization was significantly enhanced in DCs stimulated with HLCA or β-glucan-coated beads larger than 15 μm, indicating that, while many factors likely contribute to the total response, the target size was a sufficient factor for DCs to polarize T_H cells differently.

Notably, our data showed that this size-specific T_H9 polarization was dependent on Dectin-1 signaling. Unlike soluble β-glucan, which is unable to activate Dectin-1 signaling, recognition of particulate β-glucan induces formation of a “phagocytic synapse” that excludes phosphatases from receptor clusters and allows for downstream signaling and phagocytosis to proceed (Freeman et al., 2016; Goodridge et al., 2011). Internalization of the receptor via phagocytosis has been implicated in terminating signaling (Hernanz-Falcon et al., 2009). Frustrated phagocytosis via Dectin-1, a condition in which a Dectin-1 receptor and the target cannot be internalized, has been shown recently to induce neutrophil NETosis and produce extracellular reactive oxygen species to promote clearance of large pathogens such as fungal hyphae (Branzk et al., 2014; Warnatsch et al., 2017). Although there have been studies to understand the role of Dectin-1 in recognizing the size of fungi and inducing immune responses (Elder et al., 2017; Hernanz-Falcon et al., 2009), further studies are needed on how this affects T_H cell differentiation. We observed that the capacity of *C. albicans* hyphae-stimulated DCs to induce a T_H9 response requires DC Dectin-1. In contrast, Dectin-2 did not play a role in recognizing the size of *C. albicans* and inducing a T_H9 response. Collectively, these results suggest that Dectin-1 is important for recognizing the size of fungi in DCs.

A role for T_H9 cells in controlling *C. albicans* infection has been suggested (Renga et al., 2018; Schlapbach et al., 2014), although the mechanisms directing T_H9 polarization have not been clear. T_H9 differentiation induced by curdlan-stimulated DCs has been reported to

be linked to expression of TNFSF15, OX40L, and IL-33 (Chen et al., 2018; Zhao et al., 2016), but this approach required the supplemental addition of T_H9-polarizing cytokines to the culture media. We have observed that increased T_H9 polarization is promoted preferentially by Dectin-1 activation in response to large, hyphal-sized targets compared with smaller yeast-sized targets and that this occurs without supplementing any extra T_H9-polarizing cytokines.

Moreover, our data, in agreement with others, indicate that DCs stimulated with large targets induce prolonged Dectin-1 signaling due to an inability to internalize the target (Hernanz-Falcon et al., 2009). Our RNA-seq analysis revealed that different gene-expression patterns characterize DCs stimulated with small or large targets. DCs stimulated with either HLCA or large beads induced multiple genes associated with T_H9 induction. We found that four genes, *Il33, Tnsf15, Tnfsf18,* and *Tnfsf4,* were regulated by the Dectin-1 receptor but not regulated by the Dectin-2 receptor. Therefore, our observations suggest that large targets increase the duration of Dectin-1 signaling in DCs, which could be a possible mechanism to induce different gene expression in DCs stimulated with large targets compared with small targets, leading to an enhanced T_H9 response.

RNA-seq analysis underscored that there are many differences in how DCs respond differentially to yeast and hyphae that cannot be replicated by Dectin-1/β-glucan signaling alone. Hyphae triggered the regulation of hundreds of genes in DCs that were not affected by yeast, and yeast triggered the regulation of dozens of genes that were not affected by hyphae. These differences could be due to differences in ligand expression or presentation by yeast and hyphae or due to differences in small-versus large-surface signaling via receptors other than Dectin-1. Further studies will be required to understand the impacts of these differential responses on host defense against fungal infection. That the subset of differential responses replicated by Dectin-1 signaling in response to small and large beads was enriched in genes involved in DC regulation of immune responses, especially *Il33*, suggests an important role for this specific signaling in the development of effective immunity.

IL-33 acts as an amplifier of inflammation and activates various types of immune cells such as T_H cells, DCs, macrophages, neutrophils, and ILC2s (Dominguez et al., 2017; Kurowska-Stolarska et al., 2009; Le et al., 2012; Piehler et al., 2016; Schmitz et al., 2005). It has been suggested that IL-33 has both protective and destructive function in antifungal immunity (Piehler et al., 2016; Tran et al., 2015) as it induces type 2 immune responses (Lohning et al., 1998; Piehler et al., 2016; Tran et al., 2015). Recent studies have reported that IL-33 also induces polarization of T_H9 cells that produce IL-9, which once had been thought to be a T_H2-derived cytokine (Chen et al., 2018; Ramadan et al., 2017). Our *Il33* knockdown data, in agreement with others, indicate that increased expression of *Il33* is a key contributing factor in enhancing the T_H9 response in DCs stimulated with large targets. However, we cannot rule out that there are contributions from other T_H9-associated genes, such as TNF superfamily members, which were also increased in mRNA expression in DCs stimulated with large targets. *Il33* is regulated by Dectin-1 signaling through the SYK, PLC, and ERK pathways and CARD9-dependent and -independent pathways. Taken together, when IL-33 is increased in DCs through Dectin-1 with large-target stimulation, it is likely

that IL-33 activates DCs and T_H cells by autocrine and paracrine mechanisms, respectively, to potentiate T_H9 polarization. This work advances our understanding of the size recognition of DCs, highlights the role of Dectin-1 in DCs discriminating target sizes, and elucidates mechanisms of action.

Limitations of the study

While the study reveals that Dectin-1-mediated DC discrimination between small and large phagocytic targets can influence their propensity to drive T_H9 polarization, significant limitations of the work include that we have not yet evaluated the contribution of this method of discrimination on T_H polarization *in vivo* and that additional factors other than size undoubtedly contribute further to the T_H-polarization decision. We focused our studies largely on the contribution of IL-33 in T_H9 polarization, while the data suggest that additional cytokines and co-stimulatory molecules upregulated in DCs stimulated with large targets likely contribute to the full measure of T_H9 support. T_H9 responses can be challenging to detect *in vivo* due to their transient nature and the small numbers of cells.

STAR★METHODS

RESOURCE AVAILABILITY

Lead contact—Further information and requests for resources and reagents should be directed to and will be fulfilled by the lead contact, David Underhill (David.Underhill@csmc.edu).

Materials availability—Requests for resources and reagents are available from the lead contact.

Data and code availability

- All data reported in this paper will be shared by the lead contact upon request.
- This paper does not report original code.
- Any additional information required to reanalyze the data reported in this paper is available from the lead contact upon request.

EXPERIMENTAL MODEL AND SUBJECT DETAILS

Mice—Female mice 8–12 weeks of age were used for experiments. C57BL/6 mice were purchased from Jackson Laboratories (Bar Harbor, ME). Rag2$^{-/-}$OT-II TCR transgenic mice and Rag1$^{-/-}$OT-II TCR transgenic mice were purchased from Taconic Bioscience (Rensselaer, NY), *Clec7a*$^{-/-}$ and *Card9*$^{-/-}$ mice from Jackson Laboratories (Bar Harbor, ME) and *Celc6a*$^{-/-}$ (Taylor et al., 2014) were bred and housed under specific pathogen-free conditions in the Cedars-Sinai Medical Center animal facility.

METHOD DETAILS

Preparation of C. *albicans* yeast and hyphae and labeled polystyrene beads—*C. albicans* yeast (SC5314) was grown with shaking overnight at 32°C in Sabouraud dextran broth (SDB) for 2 days and hyphal *C. albicans* were grown in Dulbecco's Modified Eagle

Medium (Corning) containing 20 g/L sucrose and 10% FBS at 37°C. Mutant *C. albicans* strains, Δefg1/cph1 *C. albicans* (yeast-locked) and Δnrg1 *C. albicans* (hyphal-locked) were kindly provided by Dr. Scott G. Filler (Harbor- UCLA Medical Center, California, USA). Yeast-locked *C. albicans* were grown at 32°C and hyphae-locked *C. albicans* were grown at 37°C in SDB for 2 days. Heat killed *C. albicans* was prepared by incubating it at 80°C for 20 min as previously reported (Fischer et al., 2021). For preparation of PFA fixed *C. albicans, C. albicans* was washed with PBS and fixed with 2% PFA (Sigma-Aldrich) overnight at 4°C and washed with PBS twice. For preparation of fragmented hyphae, *C. albicans* (SN250) were first grown in DMEM medium with 10% FBS on tissue culture-treated dish overnight, then washed with PBS, collected by scraping and fixed with 2% PFA as described above. The fixed hyphae were subsequently fragmented by bead-beating for 5min (bead-ruptor 12, speed on high, with cooling on ice after each 1 min of bead-beating) and passing through 30G syringe needle right before use. 5 mL of PFA-fixed *C. albicans* or heat killed *C. albicans* or fragmented hyphae were dried in a SpeedVac and total dry weight was determined. For stimulations, the same dry weight/volume of yeast and hyphae was used. 3, 6, 15, 25, and 45 μm polystyrene beads (Polysciences) were passively labeled for 1 h at 37°C with 1 mg/mL soluble β-glucan (WGP soluble, Invivogen), mannan (Sigma-Aldrich), or BSA (Millipore) with tumbling. Beads were washed with PBS. The same surface area/volume of each bead preparation was used for DC stimulation.

DC preparation and stimulation—Mouse bone marrow derived DCs were grown as previously described (Goodridge et al., 2009). DCs were stimulated overnight with PFA-fixed yeast (10 yeast/cell), PFA-fixed hyphae (same dry weight as yeast preparation), 3,6,15, 25, and 45 μm polystyrene beads (10, 2.5, 0.4, 0.144, 0.044 beads/cell respectively). For inhibitor studies, cells were treated with U-73122 (Cayman chemical), U0126 (Tocris Bioscience), SB203580(Invivogen) or piceatannol (Selleck Chemicals) 1 h prior to addition of stimuli.

DC/OT-II T cell co-culture—2×10^4/well of DCs were plated in 96 well round-bottom plates in RPMI (Thermo Scientific) supplemented with 10% FBS, 5 ng/ml GM-CSF and stimulated with either *C. albicans* or polystyrene beads overnight. The next day, DCs were pulsed with 500 nM Ova 323–339 peptide (Anaspec) for 2 h and then co-cultured with 2×10^5 of naïve Rag1$^{-/-}$ or Rag2$^{-/-}$ OT-II TCR transgenic CD4$^+$ T cells for 3 days. Naïve CD4$^+$ T cells were isolated from spleens and axillary, brachial, inguinal, and mesenteric lymph nodes from Rag$^{-/-}$ OT-II TCR transgenic mice and purified by using an EasySep mouse naive CD4$^+$ T cell isolation kit (Stem Cell Technologies). For co-cultures with wild-type naïve CD4$^+$ T cells, 1×10^6 DCs were plated in non-tissue culture treated 12-well-plates and stimulated with either yeast of hyphal form of *C. albicans* overnight. The next day, 2×10^4 of DCs were transferred to each well of 96 well round-bottom plates and pulsed with 500 nM Ova 323–339 peptide for 2 h and then co-cultured with 2×10^5 of wild-type naïve CD4$^+$ T cells.

Cytokine measurement—Culture media was collected on day 3 of co-culture, and production of IFNγ, IL-4, IL-17A, IL-9 (all from Biolegend), or IL-13 (Thermo-Fisher)

were measured by enzyme-linked immunosorbent assay (ELSIA) according to the manufacturer's instructions.

Flow cytometry—Fluorophore-conjugated anti-mouse Dectin-1 (2A11) antibody was used to stain cells. Samples were pre-incubated with TruStain FcX (anti-CD16/CD32) (Biolegend) to block Fc receptors for 15 min in the presence of Zombie fixable viability dye (Biolegend) to discriminate dead cells. Following addition of Fc-block and viability dye, cells were stained with FITC conjugated anti-Dectin-1 antibody (Serotec) for 30 min at 4°C. Samples were acquired using an LSRII (BD biosciences), and data were analyzed with FlowJo version 10.1 (Tree star).

Microscopy—For staining β-glucan on fungal cell wall, PFA-fixed YLCA or HLCA were incubated with Protein-Free (TBS) Blocking Buffer (Pierce™) for 15 min at room temperature in a Thermomixer at 300 rpm. Fungi were then incubated with 1 μg/mL of recombinant protein, soluble murine Dectin-1 receptor fused with human IgG1 Fc domain (Invivogen) or recombinant Human IgG1 Fc (Biolegend) as a control for 1 h at room temperature in a Thermomixer at 300 rpm. After 3 washes, fungi were stained with AF-647 Goat Anti-Human IgG, Fcγ fragment specific (Jackson ImmunoResearch) for 30 min at room temperature in a Thermomixer at 300 rpm. Images were acquired with a Zeiss Cell Observer microscope system and ZEN 3.1 software (Carl Zeiss, Jena, Germany). Analysis of the raw data of the images was performed with ZEN 3.1 software (Carl Zeiss, Jena, Germany). Quantification of Dectin-1 intensity on the surface of the DCs was assessed by measuring integrated density of fluorescence signal/area with Fiji software. Data are the results of the quantification of more than 3 images.

For immunocytochemistry, DCs were plated on glass coverslips the night before imaging. PFA-fixed *C. albicans* yeast or hyphae were added to cells followed by a quick spin to ensure cell contact with fungi. After 10 min of stimulation, DCs were fixed with 4% PFA for 30 min at room temperature. Cells were permeabilized with ice-cold acetone for 10 min and stained with rabbit anti-phospho-SYK (Y525/526) (Cell Signaling), TRITC-phalloidin (Invitrogen), and DAPI. SYK phosphorylation on phagosomes was visualized using an AF-488-conjugated anti-rabbit secondary antibody (Invitrogen). Images were acquired with a Zeiss Cell Observer microscope system and Zen software. For Dectin-1 staining, 1×10^5 of DCs were plated on EZ Slides (Millipore Sigma). The next day, β-glucan-coated beads or PFA-fixed *C. albicans* yeast or hyphae were added to cells for the indicated times. DCs were fixed with 4% PFA for 15 min at room temperature and stained with anti-Dectin-1 antibody (Biorad) overnight at 4°C. Next day cells were visualized using an AF-488-conjugated anti-rat secondary antibody (Invitrogen).

Quantitative RT-PCR—Total mRNA was isolated from DCs (1×10^6 cells/sample) with TRIzol and RNeasy mini kit (Qiagen). cDNA was prepared with M-MLV reverse transcriptase (Invitrogen), and qPCR reactions were run with iTaq Universal SYBR Green or iTaq Universal Probes Supermix (both from Biorad) using a qTOWER^3 (Analytik Jena). Primers used are listed in the Key Resources Table.

RNA-seq library and sequencing—Total mRNA was purified from DCs (1×10^6 cells/sample) stimulated overnight with the indicated stimuli using a RNeasy kit (Qiagen). For RNA sequencing analysis, three biological replicates were used for each condition. Total RNA samples were assessed for concentration using the Nanodrop 8000 spectrophotometer (Thermo Scientific) and quality using the Agilent 2100 Bioanalyzer. Sample libraries are sequenced on NovaSeq 6000 (Illumina) using 150 paired-end sequencing. On average, about 40 million reads were generated from each sample.

RNA-seq data analysis—Raw reads obtained from RNA-Seq were aligned to the transcriptome using STAR (Galaxy Version 2.7.7a) on the Galaxy server (Townsend et al., 2000) with default parameters, using a custom mouse GRCm38 transcriptome reference downloaded from https://www.ncbi.nlm.nih.gov, containing all protein coding and long non-coding RNA genes based on NCBI mm10 annotation. Aligned files were imported in R (version 4.0.2), and FeatureCounts of Rsubread (version 2.2.6) was used to count the reads for each gene in all samples. Expression counts for each gene in all samples were normalized by a modified trimmed mean of the M-values normalization method and fitted into a negative binomial generalized linear model with DESeq2 (version 1.28.1). Differential expressed gene candidates were selected with DESeq2 with a false discovery rate less than 0.05 and log2 fold change greater than 2. For visualization of coordinated gene expression in samples, a two-way hierarchical clustering with Pearson correlation distance matrix was performed and differentially expressed gene candidates were visualized using ComplexHeatmap (version 2.4.3) in R. VennDiagram (version 1.6.20) in R was used to visualize overlapping genes.

Signaling analysis—For immunoblot analysis, cells were lysed in LDS sample buffer (Invitrogen) at each time point. Activation of Dectin-1 signaling pathways was measured by immunoblotting with antibodies against phospho-SYK (Y525/Y526), SYK, pERK (Thr202/Tyr204), ERK (all from Cell Signaling), and GAPDH (Santa Cruz). Immunoblots were visualized with SuperSignal West Pico Chemiluminescent Substrate (Thermo Scientific) and by exposure to autoradiography film (VWR) or with ChmiDoc (Bio-rad). ImageJ was used for quantification of the band intensity.

siRNA knockdown of *Il33*—*Il33*** mRNA was knocked down by using small interfering RNA (siRNA). FlexiTube siRNA (Qiagen) were transfected to DCs by using Neon (Invitrogen) according to the manufacturer's instruction and the most effective siRNA was chosen for the co-culture experiment. In brief, cells were washed with PBS and resuspend in buffer R at a concentration of 2×10^6 cells/100 μL. Cells were mixed with 1 μLof 100 μM siRNA prior to electroporation. DCs were rested for 1 day, pulsed with Ova peptides for 2 h, and stimulated with stimuli overnight.

QUANTIFICATION AND STATISTICAL ANALYSIS

All experiments were conducted with at least triplicate measurements a minimum of two times unless otherwise stated in the figure legends. Statistical significance was determined by ANOVA using GraphPad Prism software.

Supplementary Material

Refer to Web version on PubMed Central for supplementary material.

ACKNOWLEDGMENTS

This study was supported by NIH R01 AI071116 to D.M.U. We thank Andrea Wolf, Helen S. Goodridge, and Jose J. Limon-Tello for helpful discussions.

REFERENCES

Afgan E, Baker D, Batut B, van den Beek M, Bouvier D, Cech M, Chilton J, Clements D, Coraor N, Gruning BA, et al. (2018). The galaxy platform for accessible, reproducible and collaborative biomedical analyses: 2018 update. Nucleic Acids Res. 46, W537–W544. [PubMed: 29790989]

Angkasekwinai P, and Dong C (2021). IL-9-producing T cells: potential players in allergy and cancer. Nat. Rev. Immunol. 21, 37–48. [PubMed: 32788707]

Branzk N, Lubojemska A, Hardison SE, Wang Q, Gutierrez MG, Brown GD, and Papayannopoulos V (2014). Neutrophils sense microbe size and selectively release neutrophil extracellular traps in response to large pathogens. Nat. Immunol. 15, 1017–1025. [PubMed: 25217981]

Brown GD, and Gordon S (2001). Immune recognition. A new receptor for beta-glucans. Nature 413, 36–37.

Brown GD, Herre J, Williams DL, Willment JA, Marshall AS, and Gordon S (2003). Dectin-1 mediates the biological effects of beta-glucans. J. Exp. Med. 137, 1119–1124.

Chen H, and Boutros PC (2011). VennDiagram: a package for the generation of highly-customizable Venn and Euler diagrams in R. BMC Bioinformatics 12, 35. [PubMed: 21269502]

Chen J, Zhao Y, Jiang Y, Gao S, Wang Y, Wang D, Wang A, Yi H, Gu R, Yi Q, et al. (2018). Interleukin-33 contributes to the induction of Th9 cells and antitumor efficacy by dectin-1-activated dendritic cells. Front Immunol. 9, 1787. [PubMed: 30108595]

Cheng Z, Taylor B, Ourthiague DR, and Hoffmann A (2015). Distinct single-cell signaling characteristics are conferred by the MyD88 and TRIF pathways during TLR4 activation. Sci. Signal. 8, ra69. [PubMed: 26175492]

d'Ostiani CF, Del Sero G, Bacci A, Montagnoli C, Spreca A, Mencacci A, Ricciardi-Castagnoli P, and Romani L (2000). Dendritic cells discriminate between yeasts and hyphae of the fungus Candida albicans. Implications for initiation of T helper cell immunity in vitro and in vivo. J. Exp. Med. 191, 1661–1674. [PubMed: 10811860]

Dardalhon V, Awasthi A, Kwon H, Galileos G, Gao W, Sobel RA, Mits-doerffer M, Strom TB, Elyaman W, Ho IC, et al. (2008). IL-4 inhibits TGF-beta-induced Foxp3+ T cells and, together with TGF-beta, generates IL-9+IL-10+ Foxp3(−) effector T cells. Nat. Immunol. 9, 1347–1355. [PubMed: 18997793]

de Kleer IM, Kool M, de Bruijn MJ, Willart M, van Moorleghem J, Schuijs MJ, Plantinga M, Beyaert R, Hams E, Fallon PG, et al. (2016). Perinatal activation of the interleukin-33 pathway promotes type 2 immunity in the developing lung. Immunity 45, 1285–1298. [PubMed: 27939673]

Dominguez D, Ye C, Geng Z, Chen S, Fan J, Qin L, Long A, Wang L, Zhang Z, Zhang Y, et al. (2017). Exogenous IL-33 restores dendritic cell activation and maturation in established cancer. J. Immunol. 198, 1365–1375. [PubMed: 28011934]

Elder MJ, Webster SJ, Chee R, Williams DL, Hill Gaston JS, and Goodall JC (2017). Beta-glucan size controls dectin-1-mediated immune responses in human dendritic cells by regulating IL-1beta production. Front Immunol. 8, 791. [PubMed: 28736555]

Elyaman W, Bassil R, Bradshaw EM, Orent W, Lahoud Y, Zhu B, Radtke F, Yagita H, and Khoury SJ (2012). Notch receptors and Smad3 signaling cooperate in the induction of interleukin-9-producing T cells. Immunity 36, 623–634. [PubMed: 22503540]

Fischer J, Gresnigt MS, Werz O, Hube B, and Garscha U (2021). Candida albicans-induced leukotriene biosynthesis in neutrophils is restricted to the hyphal morphology. FASEB J. 35, e21820. [PubMed: 34569657]

Freeman SA, Goyette J, Furuya W, Woods EC, Bertozzi CR, Bergmeier W, Hinz B, van der Merwe PA, Das R, and Grinstein S (2016). Integrins form an expanding diffusional barrier that coordinates phagocytosis. Cell 164, 128–140. [PubMed: 26771488]

Fu Y, Phan QT, Luo G, Solis NV, Liu Y, Cormack BP, Edwards JE Jr., Ibrahim AS, and Filler SG (2013). Investigation of the function of Candida albicans Als3 by heterologous expression in Candida glabrata. Infect. Immun. 81, 2528–2535. [PubMed: 23630968]

Gantner BN, Simmons RM, and Underhill DM (2005). Dectin-1 mediates macrophage recognition of Candida albicans yeast but not filaments. EMBO J. 24, 1277–1286. [PubMed: 15729357]

Gerlach K, Hwang Y, Nikolaev A, Atreya R, Dornhoff H, Steiner S, Lehr HA, Wirtz S, Vieth M, Waisman A, et al. (2014). TH9 cells that express the transcription factor PU.1 drive T cell-mediated colitis via IL-9 receptor signaling in intestinal epithelial cells. Nat. Immunol. 15, 676–686. [PubMed: 24908389]

Goodridge HS, Reyes CN, Becker CA, Katsumoto TR, Ma J, Wolf AJ, Bose N, Chan AS, Magee AS, Danielson ME, et al. (2011). Activation of the innate immune receptor Dectin-1 upon formation of a 'phagocytic synapse. Nature 472, 471–475. [PubMed: 21525931]

Goodridge HS, Shimada T, Wolf AJ, Hsu YM, Becker CA, Lin X, and Underhill DM (2009). Differential use of CARD9 bydectin-1 in macrophages and dendritic cells. J. Immunol. 182, 1146–1154. [PubMed: 19124758]

Goodridge HS, Simmons RM, and Underhill DM (2007). Dectin-1 stimulation by Candida albicans yeast or zymosan triggers NFAT activation in macrophages and dendritic cells. J. Immunol. 178, 3107–3115. [PubMed: 17312158]

Gorski SA, Hahn YS, and Braciale TJ (2013). Group 2 innate lymphoid cell production of IL-5 is regulated by NKT cells during influenza virus infection. PLoS Pathog. 9, e1003615. [PubMed: 24068930]

Graham LM, Tsoni SV, Willment JA, Williams DL, Taylor PR, Gordon S, Dennehy K, and Brown GD (2006). Soluble Dectin-1 as atool to detect beta-glucans. J. Immunol. Methods 314, 164–169. [PubMed: 16844139]

Gringhuis SI, den Dunnen J, Litjens M, van der Vlist M, Wevers B, Bruijns SC, and Geijtenbeek TB (2009). Dectin-1 directs T helper cell differentiation by controlling noncanonical NF-kappaB activation through Raf-1 and Syk. Nat. Immunol. 10, 203–213. [PubMed: 19122653]

Gu Z, Eils R, and Schlesner M (2016). Complex heatmaps reveal patterns and correlations in multidimensional genomic data. Bioinformatics 32, 2847–2849. [PubMed: 27207943]

Hernanz-Falcon P, Joffre O, Williams DL, and Reis e Sousa C (2009). Internalization of Dectin-1 terminates induction of inflammatory responses. Eur. J. Immunol. 39, 507–513. [PubMed: 19130473]

Hori J, Taniguchi H, Wang M, Oshima M, and Azuma M (2010). GITR ligand-mediated local expansion of regulatory T cells and immune privilege of corneal allografts. Invest. Ophthalmol. Vis. Sci. 51, 6556–6565. [PubMed: 20702832]

Igyarto BZ, Haley K, Ortner D, Bobr A, Gerami-Nejad M, Edelson BT, Zurawski SM, Malissen B, Zurawski G, Berman J, et al. (2011). Skin-resident murine dendritic cell subsets promote distinct and opposing antigen-specific T helper cell responses. Immunity 35, 260–272. [PubMed: 21782478]

Jiang Y, Chen J, Bi E, Zhao Y, Qin T, Wang Y, Wang A, Gao S, Yi Q, and Wang S (2019). TNF-alpha enhances Th9 cell differentiation and antitumor immunity via TNFR2-dependent pathways. J. Immunother. Cancer 7, 28. [PubMed: 30717817]

Jones CP, Gregory LG, Causton B, Campbell GA, and Lloyd CM (2012). Activin A and TGF-beta promote T(H)9 cell-mediated pulmonary allergic pathology. J. Allergy Clin. Immunol. 129, 1000–1010.e1003. [PubMed: 22277204]

Joshi VB, Geary SM, and Salem AK (2013). Biodegradable particles as vaccine delivery systems: size matters. AAPS J. 15, 85–94. [PubMed: 23054976]

Kagan JC, Su T, Horng T, Chow A, Akira S, and Medzhitov R (2008). TRAM couples endocytosis of Toll-like receptor 4 to the induction of interferon-beta. Nat. Immunol. 9, 361–368. [PubMed: 18297073]

Karim AF, Reba SM, Li Q, Boom WH, and Rojas RE (2017). Toll like Receptor 2 engagement on CD4(+) T cells promotes TH9 differentiation and function. Eur. J. Immunol. 47, 1513–1524. [PubMed: 28665005]

Kashem SW, Igyarto BZ, Gerami-Nejad M, Kumamoto Y, Mohammed JA, Jarrett E, Drummond RA, Zurawski SM, Zurawski G, Berman J, et al. (2015). Candida albicans morphology and dendritic cell subsets determine T helper cell differentiation. Immunity 42, 356–366. [PubMed: 25680275]

Kurowska-Stolarska M, Stolarski B, Kewin P, Murphy G, Corrigan CJ, Ying S, Pitman N, Mirchandani A, Rana B, van Rooijen N, et al. (2009). IL-33 amplifies the polarization of alternatively activated macrophages that contribute to airway inflammation. J. Immunol. 183, 6469–6477. [PubMed: 19841166]

Le HT, Tran VG, Kim W, Kim J, Cho HR, and Kwon B (2012). IL-33 priming regulates multiple steps of the neutrophil-mediated anti-Candida albicans response by modulating TLR and dectin-1 signals. J. Immunol. 189, 287–295. [PubMed: 22661085]

LeibundGut-Landmann S, Gross O, Robinson MJ, Osorio F, Slack EC, Tsoni SV, Schweighoffer E, Tybulewicz V, Brown GD, Ruland J, et al. (2007). Syk- and CARD9-dependent coupling of innate immunity to the induction of T helper cells that produce interleukin 17. Nat. Immunol. 8, 630–638. [PubMed: 17450144]

Leleux JA, Pradhan P, and Roy K (2017). Biophysical attributes of CpG presentation control TLR9 signaling to differentially polarize systemic immune responses. Cell Rep. 18, 700–710. [PubMed: 28099848]

Liao W, Spolski R, Li P, Du N, West EE, Ren M, Mitra S, and Leonard WJ (2014a). Opposing actions of IL-2 and IL-21 on Th9 differentiation correlate with their differential regulation of BCL6 expression. Proc. Natl. Acad. Sci. USA 111,3508–3513. [PubMed: 24550509]

Liao Y, Smyth GK, and Shi W (2014b). featureCounts: an efficient general purpose program for assigning sequence reads to genomic features. Bioinformatics 30,923–930. [PubMed: 24227677]

Liao Y, Smyth GK, and Shi W (2019). The R package Rsubread is easier, faster, cheaper and better for alignment and quantification of RNA sequencing reads. Nucleic Acids Res. 47, e47. [PubMed: 30783653]

Liew FY, Girard JP, and Turnquist HR (2016). Interleukin-33 in health and disease. Nat. Rev. Immunol. 16, 676–689. [PubMed: 27640624]

Lohning M, Stroehmann A, Coyle AJ, Grogan JL, Lin S, Gutierrez-Ra-mos JC, Levinson D, Radbruch A, and Kamradt T (1998). T1/ST2 is preferentially expressed on murine Th2 cells, independent of interleukin 4, interleukin 5, and interleukin 10, and important for Th2 effector function. Proc. Natl. Acad. Sci. USA 95, 6930–6935. [PubMed: 9618516]

Love MI, Huber W, and Anders S (2014). Moderated estimation of fold change and dispersion for RNA-seq data with DESeq2. Genome Biol. 15, 550. [PubMed: 25516281]

Lowman DW, Greene RR, Bearden DW, Kruppa MD, Pottier M, Mon-teiro MA, Soldatov DV, Ensley HE, Cheng SC, Netea MG, et al. (2014). Novel structural features in Candida albicans hyphal glucan provide a basis for differential innate immune recognition of hyphae versus yeast. J. Biol. Chem. 289, 3432–3443. [PubMed: 24344127]

Mant A, Chinnery F, Elliott T, and Williams AP (2012). The pathway of cross-presentation is influenced bythe particle size of phagocytosed antigen. Immunology 136, 163–175. [PubMed: 22260486]

Marakalala MJ, Vautier S, Potrykus J, Walker LA, Shepardson KM, Hopke A, Mora-Montes HM, Kerrigan A, Netea MG, Murray GI, et al. (2013). Differential adaptation of Candida albicans *in vivo* modulates immune recognition by dectin-1. PLoS Pathog. 9, e1003315. [PubMed: 23637604]

Molofsky AB, Savage AK, and Locksley RM (2015). Interleukin-33 in tissue homeostasis, injury, and inflammation. Immunity 42, 1005–1019. [PubMed: 26084021]

Mukaremera L, Lee KK, Mora-Montes HM, and Gow NAR (2017). Candida albicans yeast, pseudohyphal, and hyphal morphogenesis differentially affects immune recognition. Front Immunol. 8, 629. [PubMed: 28638380]

Ost KS, O'Meara TR, Stephens WZ, Chiaro T, Zhou H, Penman J, Bell R, Catanzaro JR, Song D, Singh S, et al. (2021). Adaptive immunity induces mutualism between commensal eukaryotes. Nature 596, 114–118. [PubMed: 34262174]

Piehler D, Eschke M, Schulze B, Protschka M, Muller U, Grahnert A, Richter T, Heyen L, Kohler G, Brombacher F, et al. (2016). The IL-33 receptor(ST2) regulates early IL-13production in fungus-induced allergic airway inflammation. Mucosal Immunol. 9, 937–949. [PubMed: 26555705]

Ramadan A, Griesenauer B, Adom D, Kapur R, Hanenberg H, Liu C, Kaplan MH, and Paczesny S (2017). Specifically differentiated T cell subset promotes tumor immunity over fatal immunity. J. Exp. Med. 214, 3577–3596. [PubMed: 29038366]

Renga G, Moretti S, Oikonomou V, Borghi M, Zelante T, Paolicelli G, Costantini C, De Zuani M, Villella VR, Raia V, et al. (2018). IL-9 and mast cells are key players of Candida albicans commensalism and pathogenesis in the gut. Cell Rep. 23, 1767–1778. [PubMed: 29742432]

Rivera Vargas T, Humblin E, Vegran F, Ghiringhelli F, and Apetoh L (2017). TH9 cells in anti-tumor immunity. Semin. Immunopathol. 39, 39–46. [PubMed: 27832300]

Rosas M, Liddiard K, Kimberg M, Faro-Trindade I, McDonald JU, Williams DL, Brown GD, and Taylor PR (2008).The induction of inflammation bydectin-1 in vivo is dependent on myeloid cell programming and the progression of phagocytosis. J. Immunol. 181, 3549–3557. [PubMed: 18714028]

Sato K, Yang XL, Yudate T, Chung JS, Wu J, Luby-Phelps K, Kimberly RP, Underhill D, Cruz PD Jr., and Ariizumi K (2006). Dectin-2 is a pattern recognition receptor for fungi that couples with the Fc receptor gamma chain to induce innate immune responses. J. Biol. Chem. 281, 38854–38866. [PubMed: 17050534]

Schindelin J, Arganda-Carreras I, Frise E, Kaynig V, Longair M, Pietzsch T, Preibisch S, Rueden C, Saalfeld S, Schmid B, et al. (2012). Fiji: an open-source platform for biological-image analysis. Nat. Methods 9,676–682. [PubMed: 22743772]

Schlapbach C, Gehad A, Yang C, Watanabe R, Guenova E, Teague JE, Campbell L, Yawalkar N, Kupper TS, and Clark RA (2014). Human TH9 cells are skin-tropic and have autocrine and paracrine proinflammatory capacity. Sci. Transl Med. 6, 219ra218.

Schmitz J, Owyang A, Oldham E, Song Y, Murphy E, McClanahan TK, Zurawski G, Moshrefi M, Qin J, Li X, et al. (2005). IL-33, an interleukin-1-like cytokine that signals via the IL-1 receptor-related protein ST2 and induces T helper type 2-associated cytokines. Immunity 23, 479–490. [PubMed: 16286016]

Schneider CA, Rasband WS, and Eliceiri KW (2012). NIH Image to ImageJ: 25 years of image analysis. Nat. Methods 9, 671–675. [PubMed: 22930834]

Sehra S, Yao W, Nguyen ET, Glosson-Byers NL, Akhtar N, Zhou B, and Kaplan MH (2015). TH9 cells are required for tissue mast cell accumulation during allergic inflammation. J. Allergy Clin. Immunol. 136, 433–440.e431. [PubMed: 25746972]

Spadoni I, Iliev ID, Rossi G, and Rescigno M (2012). Dendritic cells produce TSLP that limits the differentiation of Th17 cells, fosters Treg development, and protects against colitis. Mucosal Immunol. 5, 184–193. [PubMed: 22236997]

Takami M, Love RB, and Iwashima M (2012).TGF-beta converts apoptotic stimuli into the signal for Th9 differentiation. J. Immunol. 188, 4369–4375. [PubMed: 22461692]

Takedatsu H, Michelsen KS, Wei B, Landers CJ, Thomas LS, Dhall D, Braun J, and Targan SR (2008). TL1A (TNFSF15) regulates the development of chronic colitis by modulating both T-helper 1 and T-helper 17 activation. Gastroenterology 135, 552–567. [PubMed: 18598698]

Tan C, Wei L, Vistica BP, Shi G, Wawrousek EF, and Gery I (2014). Phenotypes of Th lineages generated by the commonly used activation with anti-CD3/CD28 antibodies differ from those generated by the physiological activation with the specific antigen. Cell Mol Immunol 11, 305–313. [PubMed: 24583715]

Taylor PR, Roy S, Leal SM Jr., Sun Y, Howell SJ, Cobb BA, Li X, and Pearlman E (2014). Activation of neutrophils by autocrine IL-17A-IL-17RC interactions during fungal infection is regulated by IL-6, IL-23, RORgammat and dectin-2. Nat. Immunol. 15, 143–151. [PubMed: 24362892]

Townsend JM, Fallon GP, Matthews JD, Smith P, Jolin EH, and McKenzie NA (2000). IL-9-deficient mice establish fundamental roles for IL-9 in pulmonary mastocytosis and goblet cell hyperplasia but not T cell development. Immunity 13, 573–583. [PubMed: 11070175]

Tran KK, and Shen H (2009). The role of phagosomal pH on the size-dependent efficiency of cross-presentation by dendritic cells. Biomaterials30,1356–1362. [PubMed: 19091401]

Tran VG, Kim HJ, Kim J, Kang SW, Moon UJ, Cho HR, and Kwon B (2015). IL-33 enhances host tolerance to Candida albicans kidney infections through induction of IL-13 production by CD4+ T cells. J. Immunol. 194, 4871–4879. [PubMed: 25847973]

Tsuda M, Hamade H, Thomas LS, Salumbides BC, Potdar AA, Wong MH, Nunnelee JS, Stamps JT, Neutzsky-Wulff AV, Barrett RJ, et al. (2019). A role for BATF3 in TH9 differentiation and T-cell-driven mucosal pathologies. Mucosal Immunol. 12, 644–655. [PubMed: 30617301]

Underhill DM, Rossnagle E, Lowell CA, and Simmons RM (2005). Dectin-1 activates Syk tyrosine kinase in a dynamic subset of macrophages for reactive oxygen production. Blood 106, 2543–2550. [PubMed: 15956283]

Vautier S, Drummond RA, Chen K, Murray GI, Kadosh D, Brown AJ, Gow NA, MacCallum DM, Kolls JK, and Brown GD (2015). Candida albicans colonization and dissemination from the murine gastrointestinal tract: the influence of morphology and Th17 immunity. Cell Microbiol 17, 445–450. [PubMed: 25346172]

Veldhoen M, Uyttenhove C, van Snick J, Helmby H, Westendorf A, Buer J, Martin B, Wilhelm C, and Stockinger B (2008). Transforming growth factor-beta 'reprograms' the differentiation of T helper 2 cells and promotes an interleukin 9-producing subset. Nat. Immunol. 9, 1341–1346. [PubMed: 18931678]

Vornholz L, and Ruland J (2020). Physiological and pathological functions of CARD9 signaling in the innate immune system. Curr. Top Microbiol. Immunol. 429,177–203. [PubMed: 32415389]

Warnatsch A, Tsourouktsoglou TD, Branzk N, Wang Q, Reincke S, Herbst S, Gutierrez M, and Papayannopoulos V (2017). Reactive oxygen species localization programs inflammation to clear microbes of different size. Immunity 46, 421–432. [PubMed: 28314592]

Wheeler RT, Kombe D, Agarwala SD, and Fink GR (2008). Dynamic, morphotype-specific Candida albicans beta-glucan exposure during infection and drug treatment. PLoS Pathog. 4, e1000227. [PubMed: 19057660]

White SJ, Rosenbach A, Lephart P, Nguyen D, Benjamin A, Tzipori S, Whiteway M, Mecsas J, and Kumamoto CA (2007). Self-regulation of Candida albicans population size during GI colonization. PLoS Pathog. 3, e184. [PubMed: 18069889]

Whiteway M, and Oberholzer U (2004). Candida morphogenesis and host-pathogen interactions. Curr. Opin. Microbiol. 7, 350–357. [PubMed: 15358253]

Wisplinghoff H, Ebbers J, Geurtz L, Stefanik D, Major Y, Edmond MB, Wenzel RP, and Seifert H (2014). Nosocomial bloodstream infections due to Candida spp. in the USA: species distribution, clinical features and antifungal susceptibilities. Int. J. Antimicrob. Agents 43, 78–81. [PubMed: 24182454]

Witchley JN, Penumetcha P, Abon NV, Woolford CA, Mitchell AP, and Noble SM (2019). Candida albicans morphogenesis programs control the balance between gut commensalism and invasive infection. Cell Host Microbe 25, 432–43.e436. [PubMed: 30870623]

Xiao X, Balasubramanian S, Liu W, Chu X, Wang H, Taparowsky EJ, Fu YX, Choi Y, Walsh MC, and Li XC (2012). OX40 signaling favors the induction of T(H)9 cells and airway inflammation. Nat. Immunol. 13, 981–990. [PubMed: 22842344]

Xiao X, Shi X, Fan Y, Zhang X, Wu M, Lan P, Minze L, Fu YX, Ghobrial RM, Liu W, et al. (2015). GITR subverts Foxp3(+) Tregs to boost Th9 immunity through regulation of histone acetylation. Nat. Commun. 6, 8266. [PubMed: 26365427]

Xue G, Jin G, Fang J, and Lu Y (2019). IL-4 together with IL-1beta induces antitumor Th9 cell differentiation in the absence of TGF-beta signaling. Nat. Commun. 10, 1376. [PubMed: 30914642]

Yao W, Zhang Y, Jabeen R, Nguyen ET, Wilkes DS, Tepper RS, Kaplan MH, and Zhou B (2013). Interleukin-9 is required for allergic airway inflammation mediated by the cytokine TSLP. Immunity 38, 360–372. [PubMed: 23376058]

Zhao Y, Chu X, Chen J, Wang Y, Gao S, Jiang Y, Zhu X, Tan G, Zhao W, Yi H, et al. (2016). Dectin-1-activated dendritic cells trigger potent antitumour immunity through the induction of Th9 cells. Nat. Commun. 7, 12368. [PubMed: 27492902]

Highlights

- Dendritic cells exposed to *C. albicans* hyphae promote T_H9 responses
- *C. albicans* yeast are poor inducers of T_H9 responses
- Hyphal size and Dectin-1 are key factors in driving T_H9 responses
- Prolonged Dectin-1 signaling promotes T_H9-driving IL-33 production

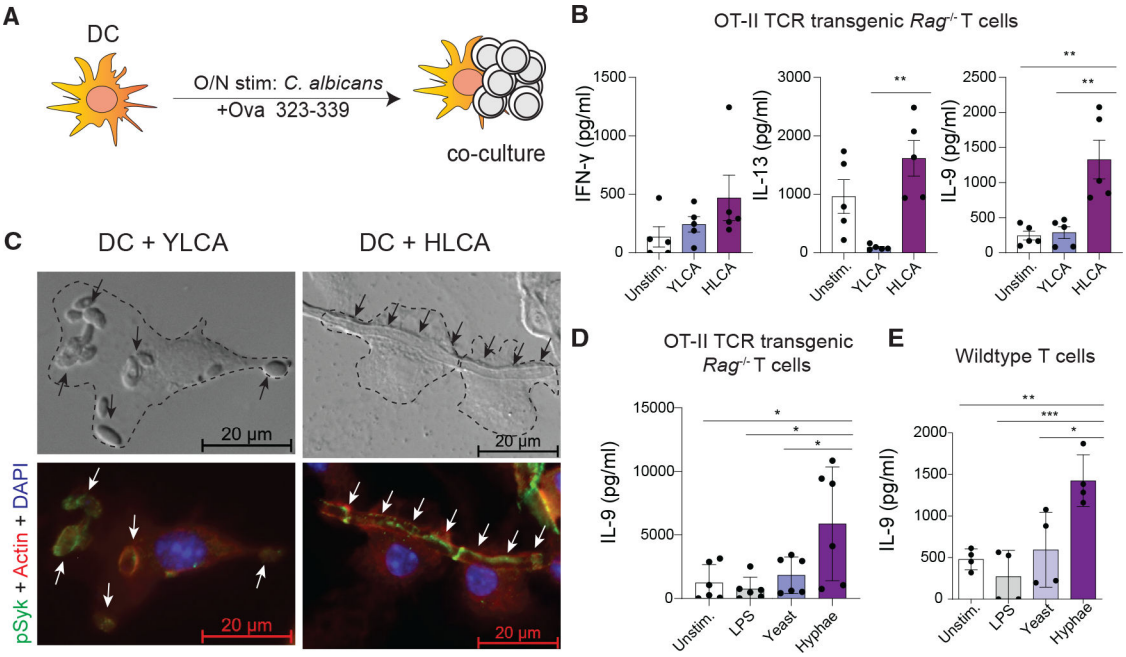

Figure 1. Different morphology of *C. albicans* induces differential activation of DCs in T_H cell polarization

(A) Experimental plan for *in vitro* DC:OT-II T cell co-culture.

(B) DCs were stimulated with yeast-locked (YLCA) or hyphae-locked (HLCA) *C. albicans,* pulsed with Ova peptide (323–339), and co-cultured with naïve *Rag*$^{-/-}$ *OT-II* CD4^{+} T cells. Production of IFNγ, IL-13, or IL-9 was assessed by ELISA. n = 5 biological replicates.

(C) Fluorescence imaging of DCs engaging *C. albicans* yeast and hyphae 10 min after addition of fungi. Phosphorylated SYK was visualized at the site of fungal contact by immunofluorescence. Actin and nuclei were visualized with phalloidin and 4',6-diamidino-2-phenylindole (DAPI), respectively. Arrows indicate locations of yeast and hyphae, and dotted line indicates edges of the DCs.

(D) DCs were stimulated with LPS, yeast or hyphal *C. albicans,* pulsed with Ova peptide (323–339), and co-cultured with naïve *Rag*$^{-/-}$ *OT-II* CD4^{+} T cells. Production of IL-9 was assessed by ELISA. n = 5 biological replicates.

(E) DCs were stimulated with LPS, yeast or hyphal *C. albicans,* and co-cultured with wild-type naïve CD4^{+} T cells. Production of IL-9 was assessed by ELISA. n = 4 biological replicates.

Results are mean ± SD analyzed using one-way ANOVA followed by Tukey's post hoc test. *$p < 0.05$, **$p < 0.005$, ***$p < 0.0005$; not significant if it is not denoted.

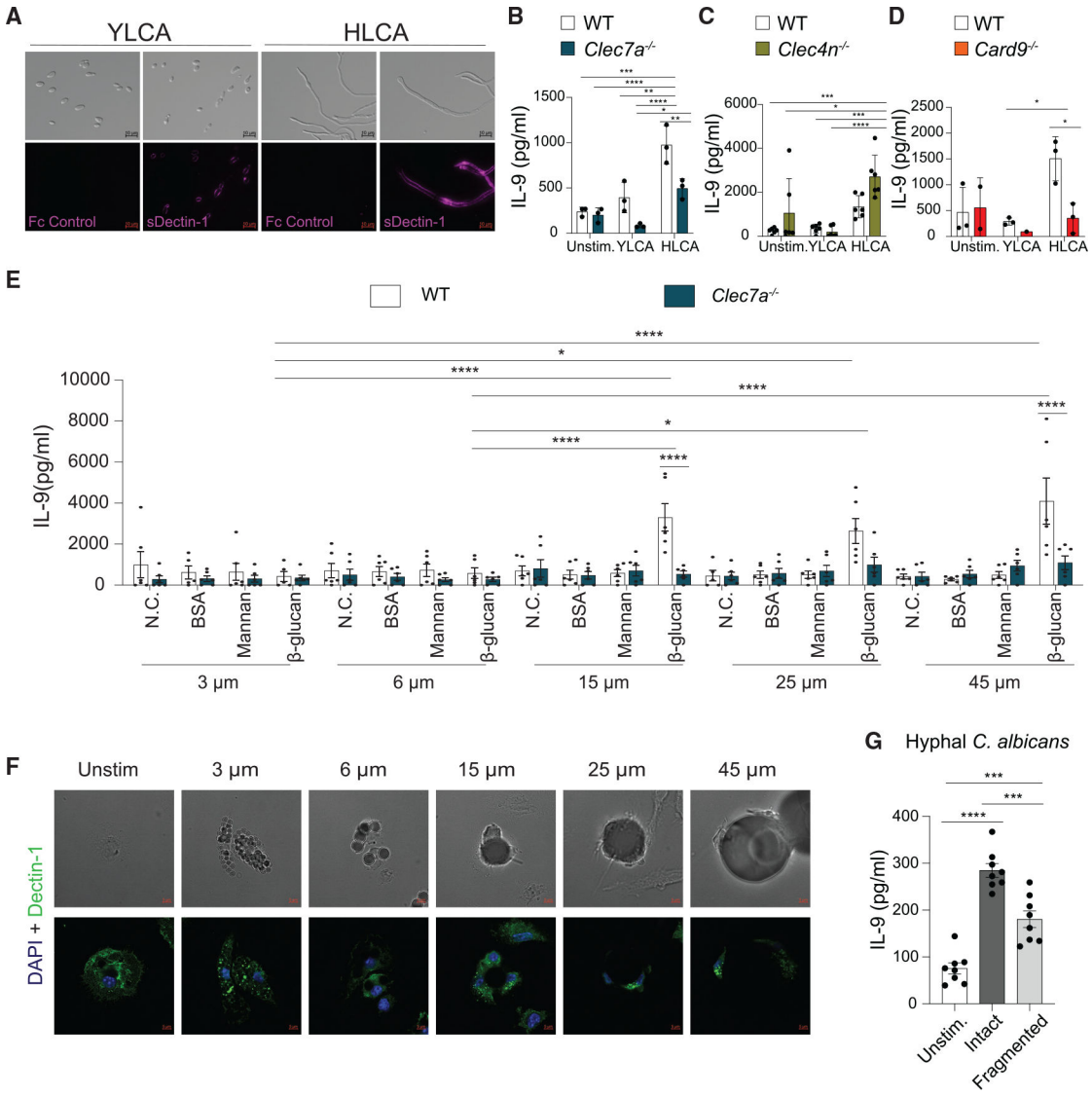

Figure 2. T_H9 polarization in DCs stimulated with large targets is dependent on Dectin-1 and CARD9

(A) Fluorescence imaging of YLCA or HLCA. β-glucan was visualized with soluble murine Dectin-1 receptor fused to human IgG1 Fc(sDectin-1),and recombinant human IgG1 Fc was used as a control.

(B–D) Wild-type or (B) Clec7a$^{-/-}$, (C) Clec4n$^{-/-}$, or (D) Card9$^{-/-}$ DCs were stimulated with YLCA or HLCA, pulsed with Ova peptide (323–339), and co-cultured with naïve Rag$^{-/-}$ OT-II CD4^{+} T cells. Production of IL-9 was assessed by ELISA. (B and D) n = 3 biological replicates. (C) n = 6 biological replicates.

(E) Wild-type or *Clec7a*$^{-/-}$ DCs were stimulated with 3, 6, 15, 25, or 45 μm polystyrene beads that were coated with BSA, mannan, or β-glucan overnight and pulsed with Ova peptide (323–339) for 2 h prior to being co-cultured with naïve *Rag*$^{-/-}$ *OT-II* CD4^{+} T cells. Production of IL-9 was assessed by ELISA. n = 6 biological replicates.

(F) Confocal images showing how DCs process the beads according to their size. DCs were stimulated with β-glucan-coated beads overnight and were stained with Dectin-1 and DAPI.

(G) Wild-type DCs were stimulated with intact or fragmented wild-type hyphal *C. albicans,* pulsed with Ova peptide (323–339), and co-cultured with naïve *Rag OT-II* $CD4^+$ T cells. Production of IL-9 was assessed by ELISA. n = 8 biological replicates.

Results are (B–D) mean ± SD or(E) mean ± SEM analyzed using two-way ANOVA followed by Tukey's post hoc test. In(E), statistical comparisons are only shown for β-glucan-coated beads of various sizes and between genotypes. *p < 0.05, **p < 0.005, ***p < 0.0005, ****p < 0.0001; not significant if it is not denoted.

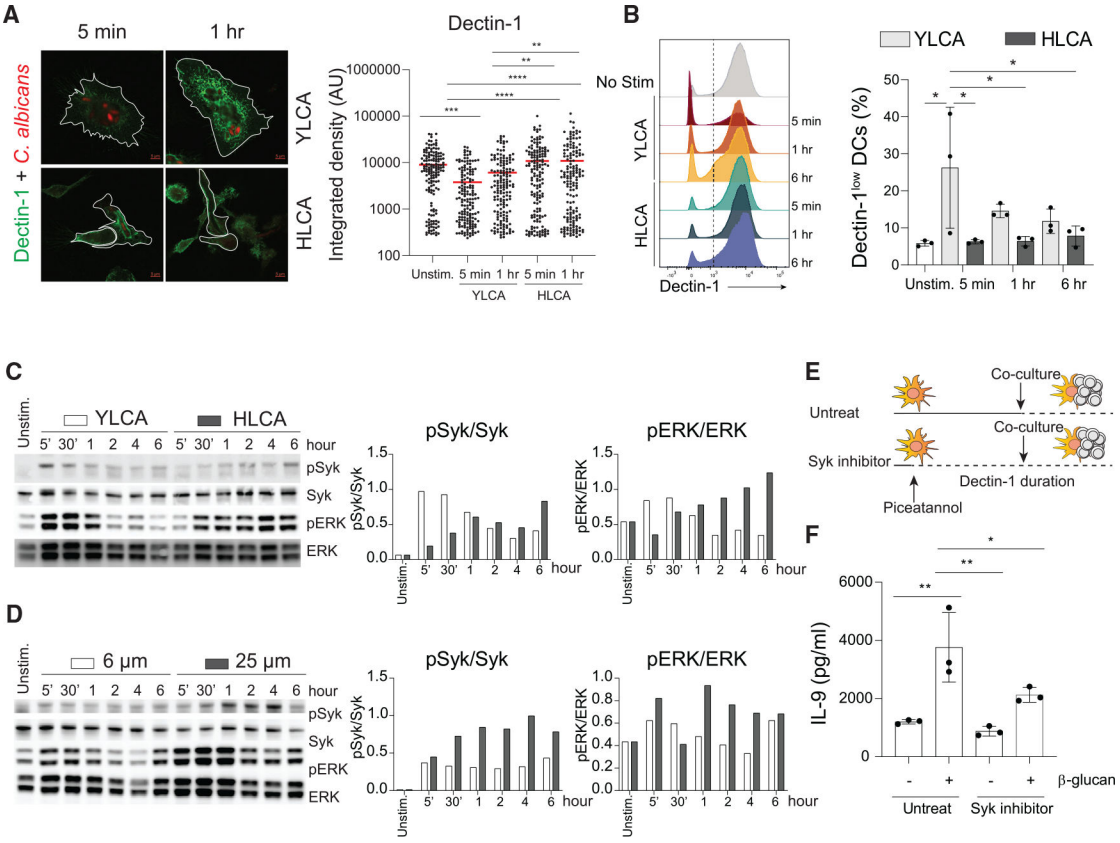

Figure 3. Duration of Dectin-1 signaling between small- versus large-target-stimulated DCs

(A) Confocal images showing surface Dectin-1 expression of DCs 5 min or 1 h after stimulating DCs with propidium-iodide-stained YLCA or HLCA (left). Relative quantification of the mean integrated density of Dectin-1 signal (right). n = 158 cells.

(B) DCs were stimulated with YLCA or HLCA for 5 min or 1 or 6 h. After stimulation, DCs were stained with fluorescein isothiocyanate (FITC)-labeled anti-Dectin-1 antibody. Representative histograms (left) show surface expression of Dectin-1 in DCs. Pooled percentages of Dectin-1^{low} DCs from 3 independent experiments are shown (right). n = 3 biological replicates.

(C–D) Representative immunoblots showing phosphorylation of SYK and ERK in DCs that were stimulated for 5 or 30 min or 1,2,4, or 6 h with (C) YLCA or HLCA or (D) β-glucan-coated polystyrene beads (6 or 25 μm) (left). Quantification of phosphorylation of SYK and ERK (right). Data are representative of more than three independent experiments.

(E) Experimental plan for *in vitro* DC:OT-II T cell co-culture. Solid line represents persistent Dectin-1 signaling, and dotted line represents inhibited Dectin-1 signaling.

(F) DCs were stimulated with a β-glucan-coated plate for 1 h and treated with an SYK inhibitor (25 μM piceatannol) overnight. The next day, DCs were transferred to a fresh plate not coated with β-glucan and co-cultured with naïve *Rag*$^{-/-}$ *OT-II* CD4^{+} T cells. Production of IL-9 was assessed by ELISA. n = 3 biological replicates.

Results are mean ± SD analyzed using one-way ANOVA followed by Tukey's post hoc test. *p < 0.05, **p < 0.005, ***p < 0.0005, ****p < 0.0001; not significant if it is not denoted.

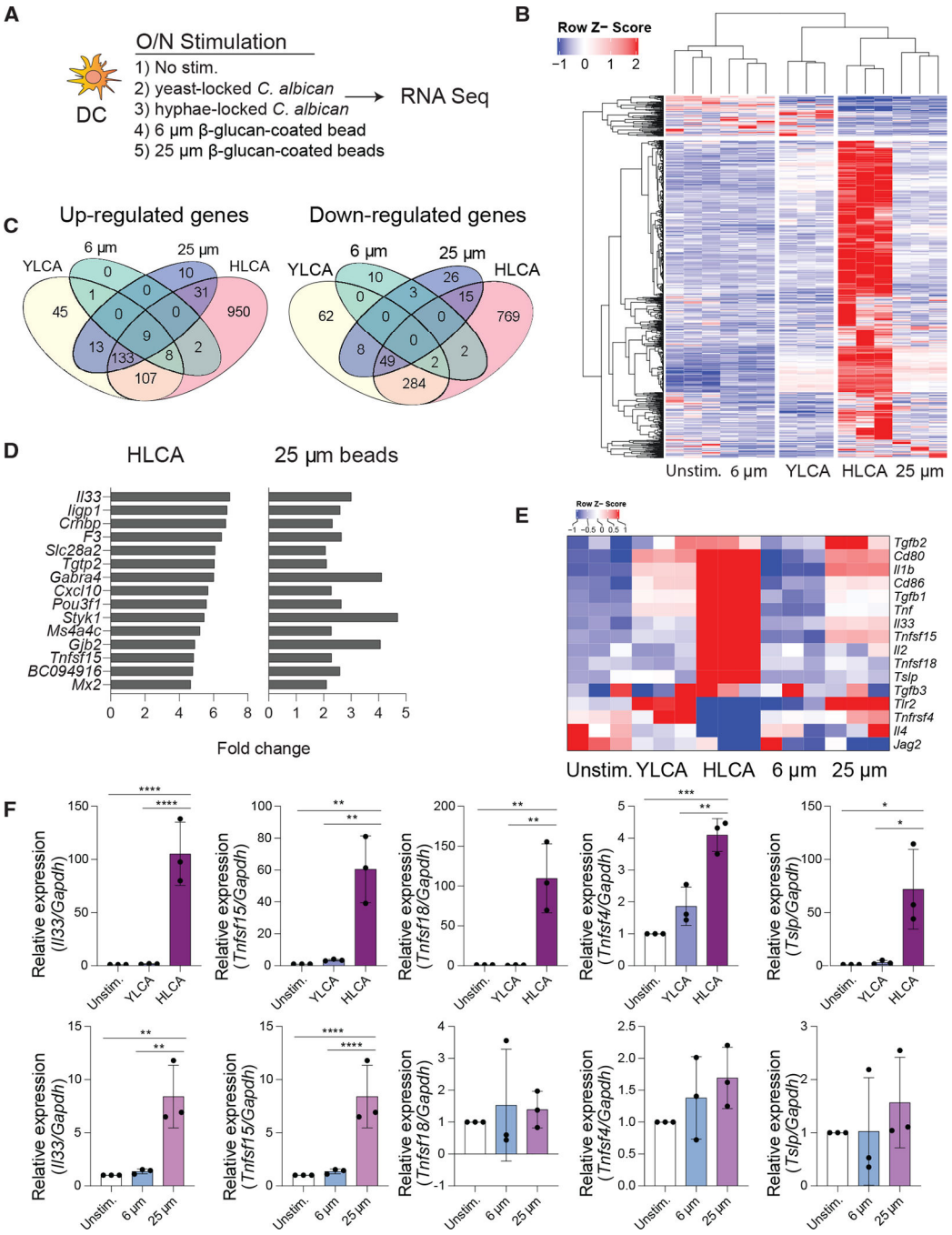

Figure 4. Transcriptome analysis of DCs stimulated with large targets reveals a transcriptional signature favoring T_H9 differentiation

(A) Experimental plan for DC activation and RNA-seq analysis.

(B) Heatmap depicting genes that are differentially expressed between DCs stimulated with small targets (β-glucan-coated 6 μm polystyrene beads or YLCA) and large targets (β-glucan-coated 25 μm polystyrene beads or HLCA). Down-regulated genes are shown in blue, and up-regulated genes are shown in red. Each column represents a biological replicate.

(C) Venn diagrams representing overlap of genes that are up- or down-regulated at least 2-fold relative to unstimulated DCs.
(D) Top 15 genes that are up-regulated in DCs stimulated with both β-glucan-coated 25 μm beads and HLCA.
(E) Heatmap of regulation of selected genes linked to T_H9 polarization.
(F) qRT-PCR analysis of select T_H9-associated gene transcripts. Data are represented as fold change in expression relative to unstimulated DCs. Genes are normalized to *Gapdh* transcript levels. n = 3 biological replicates.
Mean ± SD analyzed using one-way ANOVA followed by Tukey's post hoc test. *$p < 0.05$, **$p < 0.005$, ***$p < 0.0005$, ****$p < 0.0001$; not Significant if it is not denoted.

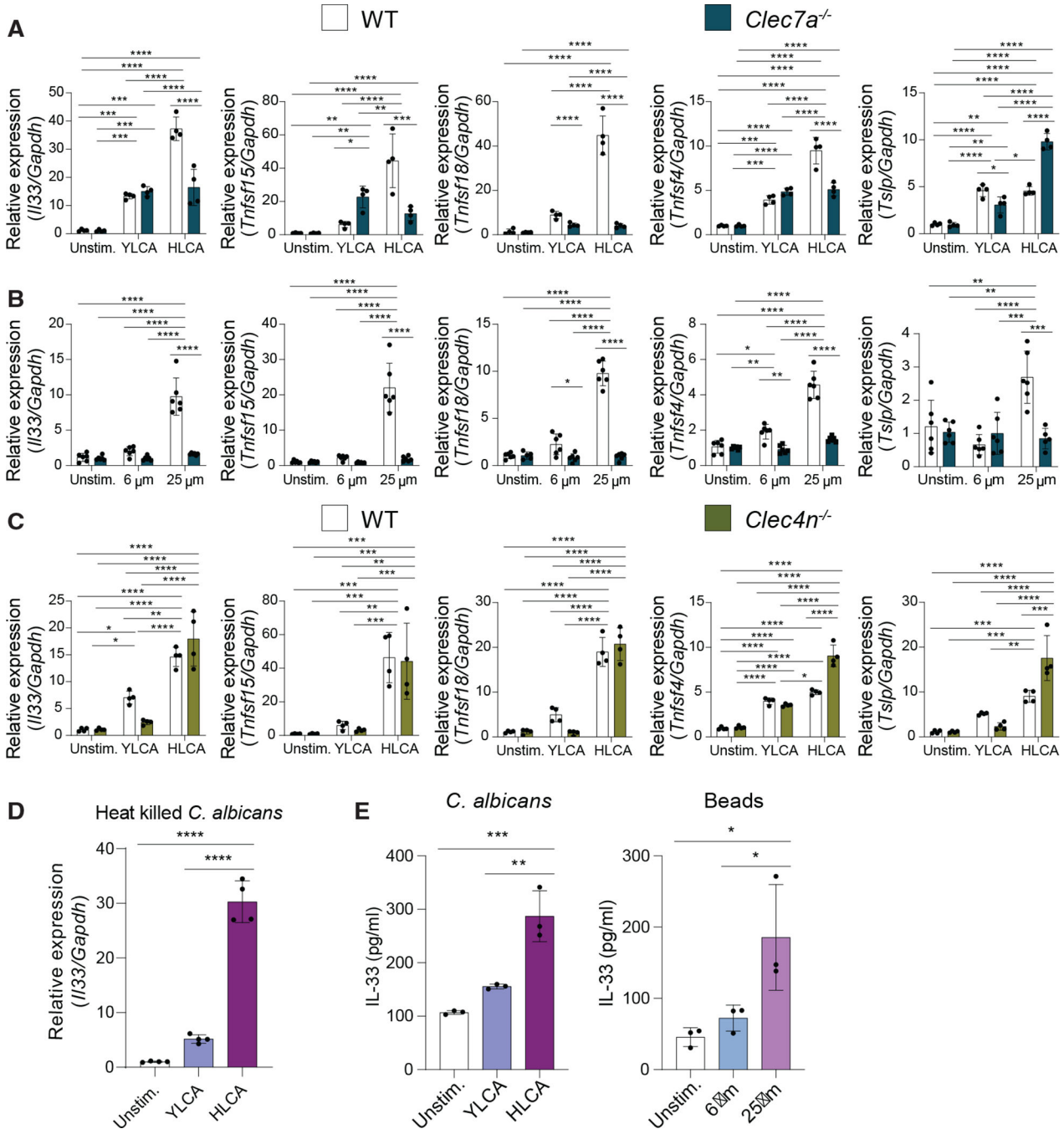

Figure 5. Increased expression of *Il33* and key *Tnfsf* members in DCs stimulated with large targets is regulated by Dectin-1 but not by Dectin-2

(A–C) Wild-type and (A and B) Clec7a$^{-/-}$ or (C) Clec4n$^{-/-}$ DCs were stimulated overnight with (A and C) YLCA or HLCA or (B) β-glucan-coated 6 μm or 25 μm polystyrene beads. mRNA expression of selected cytokines driving T_H9 differentiation was assessed by qRT-PCR. n = 4 biological replicates.

(D) Wild-type DCs were stimulated with heat-killed YLCA or HLCA overnight. mRNA expression of *Il33* was assessed by qRT-PCR. n = 4 biological replicates.

(E) Wild-type DCs were stimulated with YLCA or HLCA overnight. DCs were lysed, and production of IL-33 was measured by ELISA. n = 3 biological replicates.
Results are mean ± SD analyzed using (A–C) two-way ANOVA or (D and E) one-way ANOVA followed by Tukey's post hoc test. *p < 0.05, **p < 0.005, ***p < 0.0005, ****p < 0.0001; not significant if it is not denoted.

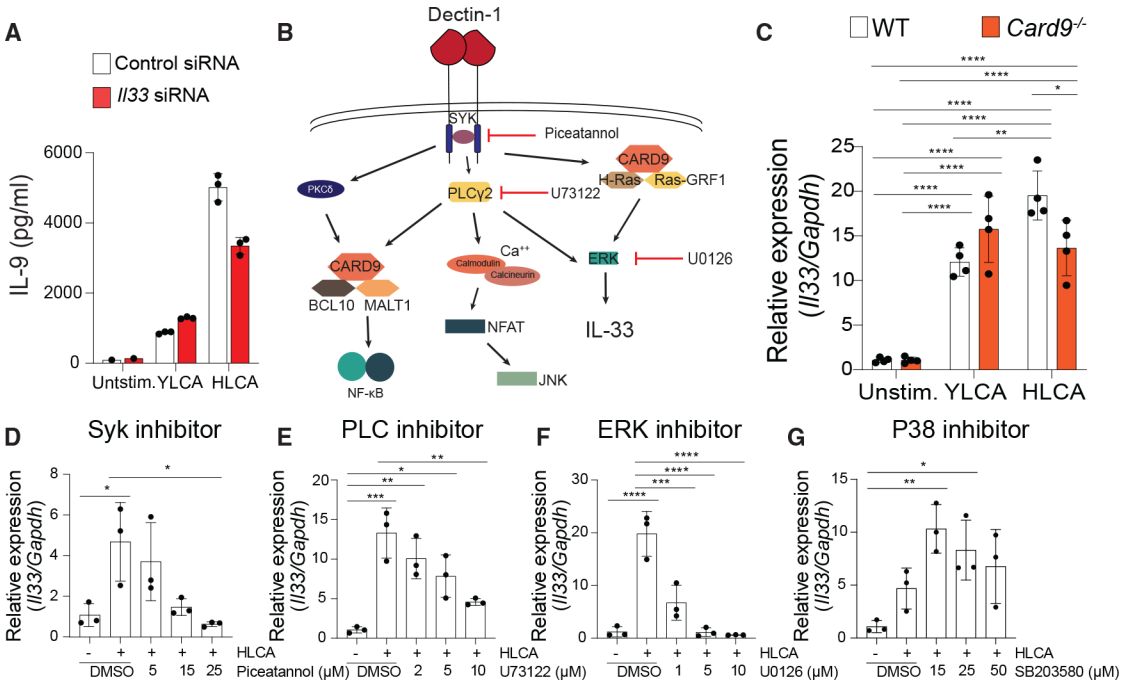

Figure 6. IL-33 is a key cytokine driving T_H9 polarization induced by DCs stimulated with large targets

(A) After transfecting *Il33* siRNAs, DCs were stimulated with YLCA or HLCA overnight and pulsed with Ova peptide (323–339) for 2 h prior to being co-cultured with naïve *Rag*$^{-/-}$ *OT-II* CD4^{+} T cells. Production of IL-9 was assessed by ELISA on day 3 of co-culture. Dots represent independent co-cultures. Data are representative data of 3 independent experiments.

(B) Schematic diagram of Dectin-1 signaling pathway and inhibitors of downstream proteins of Dectin-1 signaling.

(C) Wild-type and CARD9-deficient DCs were stimulated with PFA-fixed YLCA or HLCA overnight, and the expression of *Il33* was measured by qRT-PCR and normalized to *Gapdh.* n = 4 biological replicates.

(D–G) DCs were treated with (D) Piceatannol, (E) U73122, (F) SB203580, or (G) U0126 1 h before stimulation with HLCA. The expression of *Il33* was measured by qRT-PCR and normalized to *Gapdh.* n = 3 biological replicates.

Results are mean ± SD analyzed using (B) two-way ANOVA or (D–G) one-way ANOVA followed by Tukey's post hoc test. *p < 0.05, **p < 0.005, ***p < 0.0005, ****p < 0.0001; not significant if it is not denoted.

KEY RESOURCES TABLE

REAGENT or RESOURCE	SOURCE	IDENTIFIER
Antibodies		
Alexa Fluor® 647 AffiniPure Goat Anti-Human IgG, Fcγ fragment specific	Jackson ImmunoResearch	Cat# 109-605-098; RRID: AB_2337889
anti-mouse Dectin-1	Bio-rad	Cat# MCA2289GA; RRID: AB_324905
FITC conjugated anti-Dectin-1 antibody	Bio-rad	Cat#MCA2289FA; RRID: AB_566381
GAPDH (6C5) antibody	Santa Cruz Biotechnology	Cat# sc-32233; RRID: AB_627679
Goat Anti-Rabbit IgG (H+L) Antibody, Alexa Fluor 488 Conjugated	Invitrogen	Cat# A-11008; RRID: AB_143165
p44/42 MAP kinase (phosphorylated Erk1/2) antibody	Cell Signaling Technology	Cat# 9101; RRID: AB_331646
p44/42 MAPK (Erk1/2) Antibody	Cell Signaling Technology	Cat# 9102; RRID: AB_330744
Phospho-Syk (Tyr525/526) (C87C1) Rabbit mAb antibody	Cell Signaling Technology	Cat# 2710; RRID: AB_2197222
Syk Antibody	Cell Signaling Technology	Cat# 2712; RRID: AB_2197223
TruStain FcX(TM) (anti-mouse CD16/32) antibody	BioLegend	Cat# 101319; RRID: AB_1574973
Bacterial and virus strains		
C. albicans (SC5314)	(Kashem et al., 2015)	N/A
C. albicans (SN250)	(Chen and Boutros, 2011)	N/A
Δefg1/cph1 *C. albicans* (yeast-locked)	(Fu et al., 2013)	N/A
Δnrg1 *C. albicans* (hyphal-locked)	(Chen and Boutros, 2011)	N/A
Chemicals, peptides, and recombinant proteins		
Corning™ Dulbecco's Modification of Eagle's Medium (DMEM)	Fisher Scientific	Cat# MT15017CV
DAPI	Sigma-Aldrich	Cat# D9542
Fetal Bovine Serum	Sigma-Aldrich	Cat# F3018
Gibco™ RPMI 1640 Medium, no glucose	Fisher Scientific	Cat# 11-879-020
iTaq™ Universal Probes Supermix	Bio-rad	Cat# 1725132
iTaq™ Universal SYBR® Green Supermix	Bio-rad	Cat# 1725122
KODAK® BioMax® Maximum Resolution (MR) Autoradiography Film	VWR	Cat# IB-IB8701302
M-MLV Reverse Transcriptase (200 U/μL)	Invitrogen	Cat# 28025013
Mannan from Saccharomyces cerevisiae	Sigma-Aldrich	Cat# M7504
NuPAGE™ LDS Sample Buffer	Invitrogen	Cat# NP0007
Ova 323-339 peptide	Anaspec	Cat# AS-27024; CAS: 92915-79-2
p38 MAP Kinase Inhibitor (SB203580)	Invivogen	Cat# tlrl-sb20; CAS: 152121-47-6
Paraformaldehyde	Sigma-Aldrich	Cat# 158127
Piceatannol	Selleck Chemicals	Cat# S3026; CAS: 10083-24-6
Pierce™ Protein-Free T20 (TBS) Blocking Buffer	Thermo Fisher Scientific	Cat# 37571
Polybead® Microspheres 15.00μm	Polysciences	Cat# 18328
Polybead® Microspheres 25.00μm	Polysciences	Cat# 07313

REAGENT or RESOURCE	SOURCE	IDENTIFIER
Polybead® Microspheres 3.00μm	Polysciences	Cat# 17134
Polybead® Microspheres 45.00μm	Polysciences	Cat# 07314
Polybead® Microspheres 6.00μm	Polysciences	Cat# 07312
Probumin® Bovine Serum Albumin Diagnostic Grade, Powder	Sigma-Aldrich	Cat# 820451
Recombinant Human IgG1 Fc (Thr106-Lys330) (carrier-free)	Biolegend	Cat# 773006
Recombinant Murine GM-CSF	Peprotech	Cat# 315-03; Accession# P01587
Rhodamine Phalloidin	Invitrogen	Cat# R415
Soluble murine Dectin-1 receptor	Invivogen	Cat# fc-mdec1a
SuperSignal™ West Pico PLUS Chemiluminescent Substrate	Thermo Fisher Scientific	Cat# 34580
TRIzol™ Reagent	Invitrogen	Cat# 15596018
U-73122	Cayman Chemical	Cat# 70740; CAS: 112648-68-7
U0126	Tocris Bioscience	Cat# 1144; CAS: 109511-58-2
WGP control / Dectin-1 inhibitor (soluble β-glucan)	Invivogen	Cat# tlrl-wgps
Zombie Violet™ Fixable Viability Kit	Biolegend	Cat# 423113
Critical commercial assays		
EasySep™ Mouse Naïve CD4+ T Cell Isolation Kit	Stem Cell Technologies	Cat# 19765
ELISA MAX™ Deluxe Set Mouse IL-4	Biolegend	Cat# 431106
ELISA MAX™ Deluxe Set Mouse IL-9	Biolegend	Cat# 442704
ELISA MAX™ Standard Set Mouse IFN-γ	Biolegend	Cat# 430802
ELISA MAX™ Standard Set Mouse IL-17A	Biolegend	Cat# 432503
ELISA MAX™ Standard Set Mouse IL-6	Biolegend	Cat# 431303
ELISA MAX™ Standard Set Mouse TNF-α	Biolegend	Cat# 430903
IL-13 Mouse Uncoated ELISA Kit	Invitrogen	Cat# 88-7137-88
RNeasy Mini Kit	Qiagen	Cat# 74106
Deposited data		
Raw and analyzed data	This paper	GEO: GSE181734
Experimental models: Organisms/strains		
C57BL/6J	Jackson Laboratories	Strain# 000664; RRID:IMSR_JAX:000664
Card9$^{-/-}$; B6.129-Card9tm1Xlin/J	Jackson Laboratories	Strain #028652; RRID: IMSR_JAX:028652
Celc6a$^{-/-}$	(Taylor et al., 2014)	MGI:4459637
Clec7a$^{-/-}$; B6.129S6-Clec7atm1Gdb/J	Jackson Laboratories	Strain #012337; RRID: IMSR_JAX:012337
Rag1$^{-/-}$OT-II TCR; B6.129S7-Rag1tm1Mom Tg(TcraTcrb)425Cbn	Taconic Bioscience	Model# 4234; RRID:IMSR_TAC:4234
Rag2$^{-/-}$OT-II TCR; B6.129S6-Rag2tm1Fwa Tg(TcraTcrb)425Cbn	Taconic Bioscience	Model# 1896; RRID:IMSR_TAC:1896
Oligonucleotides		

REAGENT or RESOURCE	SOURCE	IDENTIFIER
For Custom Primer Sequences, see Table S1		
FlexiTube GeneSolution GS77125 for Il33	Qiagen GeneGlobe	Cat# 1027416; GeneGlobe Id: GS77125
Software and algorithms		
ComplexHeatmap (version 2.4.3)	(Gu et al., 2016)	RRID:SCR_017270; https://bioconductor.org/packages/release/bioc/html/ComplexHeatmap.html
DESeq2 (version 1.28.1).	(Love et al., 2014)	RRID:SCR_015687; https://bioconductor.org/packages/release/bioc/html/DESeq2.html
FeatureCounts	(Liao et al., 2014b)	RRID:SCR_012919; http://bioinf.wehi.edu.au/featureCounts/
Fiji	(Schindelin et al., 2012)	RRID:SCR_002285; https://imagej.net/software/fiji/
FlowJo version 10.1 (Tree star).	BD biosciences	https://www.flowjo.com/solutions/flowjo/downloads
Image J	(Schneider et al., 2012)	RRID:SCR_003070; https://imagej.net/
Image Lab	Bio-rad	https://www.bio-rad.com/en-us/product/image-lab-software?ID=KRE6P5E8Z
qPCRsoft 3.4	Analytik Jena	RRID:SCR_021910; https://www.analytik-jena.com/products/life-science/pcr-qpcr-thermal-cycler/real-time-thermal-cycler-qpcr/qtower3-series/
R (version 4.0.2)	R	https://www.r-project.org/
Rsubread (version 2.2.6)	(Liao et al., 2019)	RRID:SCR_009803; http://subread.sourceforge.net/
STAR (Galaxy Version 2.7.7a)	(Afgan et al., 2018)	https://usegalaxy.org
VennDiagram (version 1.6.20)	(Chen and Boutros, 2011)	RRID:SCR_002414; http://cran.r-project.org/web/packages/VennDiagram/
ZEN 3.1	ZEISS	RRID:SCR_013672; https://www.zeiss.com/microscopy/us/products/microscope-software/zen-lite.html